2022

Rescue of sleep-dependent brain rhythm function to slow Alzheimer’s disease

BOSTON UNIVERSITY

SCHOOL OF MEDICINE

Dissertation

RESCUE OF SLEEP-DEPENDENT BRAIN RHYTHM FUNCTION TO SLOW ALZHEIMER'S DISEASE

by

YEE FUN LEE

B.S., National Chung Hsing University, Taiwan, 2007
M.S., National Chung Hsing University, Taiwan, 2010

Submitted in partial fulfillment of the

requirements for the degree of

Doctor of Philosophy

2022

Approved by

First Reader

Ronald J. Killiany, Ph.D.
Professor of Anatomy & Neurobiology

Second Reader

Brian J. Bacskai, Ph.D.
Professor of Neurology
Harvard Medical School/Massachusetts General Hospital

Third Reader

Ksenia V. Kastanenka, Ph.D.
Assistant Professor of Neurology
Harvard Medical School/Massachusetts General Hospital

DEDICATION

I would like to dedicate this work to my lovely husband Chris, my wonderful child Liam, and my adorable dog Lulu.

ACKNOWLEDGMENTS

I would like to thank my PhD advisor Dr. Brian Bacskai for accepting me as his PhD student 5 years ago. He has been devoting a huge amount of time and effort to help me grow and become a good scientist. I would also like to thank Brian for his guidance and advice for my projects and his support throughout this journey. I am always grateful to learn from him and to be a part of his lab.

I would also like to thank my PhD advisor Dr. Ksenia Kastanenka for dedicating a large amount of time and effort to guide and train me to become a good scientist. I want to thank Ksenia for her training, so I could successfully conduct research experiments. In addition, I would like to thank Ksenia for her suggestions on writing my manuscripts and presenting the results. I am always thankful for all the support she gave, especially during the time when I welcomed my baby Liam.

I would also like to thank my PhD advisor Dr. Ronald Killiany for agreeing to be my advisor at BU. I am thankful for his supervision so that I could fulfill all the requirements. I also want to thank my committee members Dr. Bradley Hyman and Dr. Dmitry Gerashchenko for the suggestions, insight and guidance for my projects. I would also like to thank Dr. Karin Schon for serving as the chair of my committee. In addition, I would like to thank all the support that I received from the department.

On the other hand, I am also thankful for all the help and support from the lab members. Especially Alyssa Russ, I couldn't have finished my project without her help. Furthermore, I want to thank Jack Zhao, Megi Maci, Morgan Miller, Steve Hou, Moustafa Algamal for their contributions to the project. I would also like to thank for the

help and support from Maria Calvo Rodriguez, Susanne Van Veluw, Patricia Kelly, Ashley Scherlek, Amanda Lariviere, Rebecca Gillani, Maria Sanchez Mico, Joyce Yang, Liz Kharitonova, Sara Whiteman, Austin Synder, Caitlin Commins, and Fan ZhanYun.

Finally, I would like to thank my family for their unconditional support. I especially would like to thank my husband Chris Lim for being so supportive and caring. He not only takes care of me, but also gives the suggestions and advice I need for my projects. I would also like to thank our adorable son Liam and dog Lulu, they are always there for me whenever I need emotional support. I am also thankful for the support from my father, mother, sisters, and brothers, they are always there for me even though they are in Malaysia and Singapore.

RESCUE OF SLEEP-DEPENDENT BRAIN RHYTHM FUNCTION TO SLOW ALZHEIMER'S DISEASE

YEE FUN LEE

Boston University School of Medicine, 2022

Major Professor: Ronald J. Killiany, Ph.D. Professor of Anatomy & Neurobiology

ABSTRACT

Patients with Alzheimer's disease (AD) experience sleep disturbances, including disruption in slow-wave sleep (SWS). Slow oscillations (≤1 Hz), a brain rhythm prevalent during SWS, play a role in memory consolidation. Interestingly, patients with AD exhibit slow oscillations of low amplitude, which might contribute to their memory impairments. The mechanisms underlying slow-wave disruptions in AD remain unknown. Slow oscillations originate in the neocortex. Cortical neurons from all layers oscillate between UP and DOWN states during slow oscillations. Astrocytes are known to support neuronal circuit functions, and disruptions in astrocyte activity might contribute to slow-wave aberrations. Here, we investigated astrocytic contributions to slow-wave disruptions in an animal model of beta-amyloidosis (APP mice). First, we monitored astrocytic calcium transients to determine whether astrocytic calcium dynamics were disrupted in APP mice. Fourier transform analysis revealed that the power, but not the frequency of astrocytic calcium transients, was disrupted in young APP mice. This suggested calcium dynamic of astrocytic network was altered and might contribute to the disruption of slow waves in APP mice. Second, we used optogenetics to synchronize cortical astrocyte activity at 0.6 Hz to drive slow oscillations in APP mice.

Our results showed that optogenetic activation of ChR2-expressing astrocytes at the endogenous frequency of slow waves restored slow-wave power. Furthermore, chronic optogenetic stimulation of astrocytes at 0.6Hz for 14 or 28 days reduced amyloid plaque deposition, prevented calcium overload in neurites, and improved memory performance in APP mice. These results revealed a malfunction of the astrocytic network driving slow-wave disruptions, and suggested a novel target to restore slow-wave power in APP mice, with translational potential to treat AD.

TABLE OF CONTENTS

LIST OF FIGURES

LIST OF ABBREVIATIONS

AAVs	Adeno-associated Viral Vectors
AD	Alzheimer's disease
ADDLs	Amyloid-beta Derived Diffusible Ligands
Aβ	Amyloid-beta
AβOs	Soluble Amyloid-β Oligomers
APP	Amyloid Precursor Protein
CBA	Chicken β–actin promoter
CFP	Cyan Fluorescent Proteins
ChR2	Channelrhodopsin-2
CMOS	Complementary Metal Oxide Semiconductor
CNS	Central Nervous System
DAPI	4',6-diamidino-2-phenylindole
EEG	Electroencephalogram
FOV	Fields of View
FRET	Fluorescence Resonant Energy Transfer
GABA	Gamma-aminobutyric Acid
$GABA_A$	Gamma-aminobutyric Acid A
$GABA_B$	Gamma-aminobutyric Acid B
GFAP	Glial Fibrillary Acidic Protein
GLAST	Glutamate Aspartate Transporter
GLT-1	Glutamate Transporter-1

IACUC	Institutional Animal Care and Use Committees
Iba-1	Ionized Calcium Binding Adaptor Molecule 1
JF_{525} dye	Janelia Flour 525 dye
MCI	Mild Cognitive Impairment
MGH	Massachusetts General Hospital
NeuN	Neuronal Nuclei
NGS	Normal goat serum
nNOS	Neuronal Nitric Oxide Synthase
NREM	Non-rapid Eye Movement
NTG	non-transgenic littermate controls
PBS	Phosphate Buffer Saline
PMTs	Photomultiplier Tubes
PS1	Presenilin 1
ROIs	Regions of Interest
SEM	Standard Error of Mean
SST	Somatostatin
SWA	Slow-wave Activity
SWS	Slow-wave Sleep
tDCS	Transcranial Direct Current Stimulation
TgCM	Transgenic Conditioned Media
TMS	Transcranial Magnetic Stimulation
VSD	voltage sensitive dyes

YC 3.6	Yellow Cameleon 3.6
YFP	Yellow Fluorescent Proteins

CHAPTER ONE: INTRODUCTION AND SPECIFIC AIMS

Disruption of slow oscillations in Alzheimer's disease

Alzheimer's disease (AD) is a progressive neurodegenerative disorder and the most common cause of dementia in the elderly (Förstl & Kurz, 1999). The pathological hallmarks of AD are the presence of extracellular plaques composed of amyloid-beta (Aβ) and intracellular neurofibrillary tangles composed of the microtubule binding protein tau in the brain (Bloom, 2014; Calderon-Garcidueñas & Duyckaerts, 2018). According to the amyloid cascade hypothesis, Aβ accumulation is thought to initiate pathological events and drive the formation of pathological tau aggregates that ultimately lead to synaptic loss and cell death (Hardy & Higgins, 1992; Henstridge et al., 2019; Selkoe & Hardy, 2016), which in turn compromises neuronal circuitry. Although, the amyloid cascade hypothesis is widely debated, soluble Aβ and tau protein aggregations have been shown to lead to synaptic dysfunction and loss of synaptic density (Spires-Jones & Hyman, 2014), resulting in memory and cognitive deficits in patients with AD (DeKosky & Scheff, 1990).

Additionally, sleep disturbances manifest early in the disease progression. Patients with AD experience sleep disruptions (Bliwise et al., 1995; McCurry et al., 1999; Moran et al., 2005), including increased amounts and frequencies of nighttime wakefulness as well as daytime napping (McCurry et al., 1999; Vitiello & Prinz, 1989). Moreover, reductions of non-rapid eye movement (NREM) sleep and slow-wave activity (SWA), a brain rhythm prevalent during NREM sleep, are evident in patients with mild AD (Lucey et al., 2019; Prinz et al., 1982; Vitiello et al., 1990), in individuals with mild

cognitive impairment (MCI) (Westerberg et al., 2012), and in older adults (Lucey et al., 2019; Mander et al., 2013, 2015).

Sleep disturbances in cognitively normal older adults could predict the Aβ burden and tau accumulation later in life (Winer et al., 2019). On the other hand, Aβ and tau deposits were associated with decreased NREM SWA in cognitively normal older adults (Ju et al., 2013; Lucey et al., 2019; Mander et al., 2015; Spira et al., 2013). Decreased NREM slow oscillations (0.6–1 Hz) were associated with increased Aβ accumulation in the medial prefrontal cortex (Mander et al., 2015). Also, higher tau deposition was correlated with decreased delta power (1–4 Hz) (Lucey et al., 2019). This evidence provides strong support for a relationship between SWA disruptions and AD pathology (**Figure 1**). Interestingly, Aβ levels fluctuate with the sleep-wake cycle, elevating during wake and declining during sleep (Kang et al., 2009; Lucey et al., 2017), suggesting that sleep facilitates Aβ clearance. Importantly, SWS was reported to enhance the clearance of Aβ when compared to the waking state via the glymphatic system (Xie et al., 2013). The glymphatic system hypothesis, although still debated (Abbott et al., 2018), states that soluble Aβ is cleared along perivascular pathways, including through the glymphatic system (Iliff et al., 2012; Xie et al., 2013) that is dependent on astrocyte activity. Thus, there is accumulating evidence for a relationship between Aβ, sleep and network activity disruptions.

Slow-wave activity and sleep-dependent memory consolidation

Human NREM sleep is subdivided into stages N1–N3 (previously stages 1–4) and is defined by the electroencephalogram (EEG) activity as synchronous waveforms,

including sleep spindles (12–14 Hz), K-complexes in stage 2 as well as slow (<1 Hz) and delta (1–4 Hz) activity in stage 3 (Iber et al., 2007). Slow and delta oscillations or isolated slow waves are commonly called SWA (Timofeev et al., 2020). Stage N3, also referred to as Delta Sleep or SWS, is characterized by the high amounts of SWA (Carskadon and Dement, 2011). During slow oscillations, excitatory and inhibitory neocortical neurons from all layers (unknown for layer 1) in anesthetized (Steriade, Contreras, et al., 1993; Steriade, Nuñez, et al., 1993a, 1993b) and sleeping animals (Chauvette et al., 2010; Steriade et al., 2001; Timofeev, Grenier, & Steriade, 2000; Timofeev et al., 2001) oscillate between depolarized (active or UP) and hyperpolarized (mostly silent or DOWN) states. Despite involvement of the entire thalamocortical system (Contreras & Steriade, 1995; Sheroziya & Timofeev, 2014; Steriade, Contreras, et al., 1993), the slow oscillations originate in neocortex and can be recorded in neocortical slices (Sanchez-Vives et al., 2010; Sanchez-Vives & McCormick, 2000), cortical cell cultures (Hinard et al., 2012; Sun et al., 2010) and isolated cortical slabs maintained *in vivo* on cats (Lemieux et al., 2014; Timofeev, Grenier, Bazhenov, et al., 2000). Slow oscillations absent from the thalamus of decorticated animals (Timofeev et al., 1996). The silent (hyperpolarized or DOWN) states of slow oscillations are periods of disfacilitation, i.e., absence of synaptic activity. Leak currents primary mediate silent states (Timofeev et al., 1996, 2001). The active (depolarized or up) states are mediated by barrages of excitatory and inhibitory synaptic activities at the level of soma (Rudolph et al., 2007; Steriade et al., 2001; Timofeev et al., 2001) and major calcium activities in dendrites (Milojkovic et al., 2007; Seibt et al., 2017). Neocortex generates slow

oscillations while thalamus contributes to their maintenance as thalamic inactivation temporally modifies cortical SWA (David et al., 2013; Lemieux et al., 2014).

To control the slow oscillations, it is important to understand the major cellular events taking place during SWA. The neuronal firing and thus synaptic activity in local cortical networks, is essentially absent in the silent state. Two major mechanisms for the active state onset are proposed. (i) The silent state is partially mediated by calcium- and sodium -dependent potassium currents. A reduction in these currents leads to the onset of a new active state (Sanchez-Vives & McCormick, 2000). (ii) Silent states are characterized by the absence of synaptic activity, but spike- independent neurotransmitter release (miniature postsynaptic potentials, minis) are still present. Co-occurrence of minis in large neurons that possess a high number of postsynaptic sites can lead to significant depolarizations and initiations of spikes, that would drive the whole network into an active state (Bazhenov et al., 2002; Chauvette et al., 2010; Timofeev, Grenier, Bazhenov, et al., 2000). Since this is a stochastic process, it can start in any cell, but more often, it starts in larger neurons, typically layer 5 large cortical pyramidal cells in experimental animals (Chauvette et al., 2010; Fiáth et al., 2016). In humans, however, slow-wave active states more often start in layer 3 (Cash et al., 2009; Csercsa et al., 2010). There might be two reasons for this difference: (a) human pyramidal cells from layer 3 are very large (Mohan et al., 2015), and therefore, they are well situated to summate minis and to trigger active states; and (b) enhanced electrical compartmentalization in layer 5 pyramidal neurons in humans does not allow dendritic depolarizing events to reach soma, even in the presence of dendritic spikes (Beaulieu-Laroche et al., 2018), therefore

reducing overall implication of layer 5 cells in network operation. Local origin of active states and dense synaptic interactions in the cortex trigger propagation of slow waves across cortical mantle (Massimini et al., 2004; Sheroziya & Timofeev, 2014; Volgushev et al., 2006). Active states are mediated by interactions of excitatory and inhibitory conductance (J.-Y. Chen et al., 2012; Haider et al., 2006; Haider & McCormick, 2009) with overall stronger inhibition at the level of soma (Haider et al., 2013; Rudolph et al., 2007). A termination of active states and transition to silent states occurs due to several factors: (i) activation of sodium - and calcium - dependent potassium currents (Sanchez-Vives & McCormick, 2000), (ii) synaptic depression (Timofeev, Grenier, & Steriade, 2000), and (iii) synchronous active inhibitory drive (Lemieux et al., 2015; Steriade, Nuñez, et al., 1993a). Because active states terminate nearly simultaneously across large cortical territories (Sheroziya & Timofeev, 2014; Volgushev et al., 2006), intrinsic current activation or synaptic depression likely do not play a leading role, because they are cell specific. Thus, we suggest that active inhibitory mechanisms terminate active states and provide network-wide synchronous onset of silent states. First, somatostatin-positive GABAergic interneurons increase activity prior to the onset of silent states (Funk et al., 2017; Niethard et al., 2018). Most of these interneurons have short axons, therefore an external trigger, possibly from thalamus, synchronizes them. Indeed, thalamic inactivation abolishes synchronous onset of silent states (Lemieux et al., 2015). Furthermore, some thalamocortical neurons fire during silent states driving parvalbumin-positive interneurons (Zucca et al., 2019). Another potential source is claustrum, the structure that has widespread cortical projections and, if activated optogenetically,

induces cortical down states (Narikiyo et al., 2020). It appears that claustrum is well situated to drive simultaneously cortical interneurons across different areas just prior to the onset of silent states.

Sleep slow oscillations play an important role in cortical plasticity. However, the direction of these plastic changes is still under discussion. A subset of studies, based mainly on indirect measurements, propose that cortical synaptic connections are strengthened during wakefulness and are weakened during sleep (Tononi & Cirelli, 2003, 2014). Other studies demonstrate that slow oscillations and overall sleep strengthens efficacy of cortical synapses (Aton et al., 2009; Chauvette et al., 2012; Jasinska et al., 2015; Seibt et al., 2012; Timofeev & Chauvette, 2017; Yang et al., 2014). Finally, there is an attempt to reach agreement in this debate which proposes that some synapses are upregulated and others are downregulated by sleep (Seibt & Frank, 2019). Irrespective of the synaptic mechanisms, sleep mediates several forms of memory consolidation (Born & Wilhelm, 2012; Diekelmann & Born, 2010; Rasch & Born, 2013). Sleep disturbances are correlated with deteriorated memory function and cognitive decline in AD and MCI patients (Brzecka et al., 2018; Moe et al., 1995). Increased night-time wakefulness and decreased slow-wave sleep (SWS), which is dominated by SWA, was associated with impaired memory and cognitive functions (Moe et al., 1995).

Slow oscillations play an important role in sleep-dependent declarative memory consolidation (Lu & Göder, 2012; Marshall et al., 2006; Steriade & Timofeev, 2003; Walker, 2009). Born and colleagues proposed a model of declarative, hippocampus-related memory consolidation during SWS. Cortical slow oscillations drive the

reactivation of short-term hippocampal memories by synchronizing hippocampal sharp wave ripples with spindle activity in the thalamus during slow oscillation UP states. This mechanism thereby contributes to the long-term synaptic plasticity changes in neocortical networks and supports the consolidation of long-term memory in neocortex (Diekelmann & Born, 2010; Rasch & Born, 2013). SWS declines with increasing age especially after the age of 30 (Van Cauter et al., 2000). Age-related reduction in SWS was correlated with impaired sleep-associated memory consolidation (Backhaus et al., 2007). Furthermore, insomnia patients with less SWS showed declines in overnight declarative memory consolidation compared to age-matched controls (Backhaus et al., 2006). Furthermore, aberrations in SWA correlated with disrupted memory consolidation in MCI patients (Westerberg et al., 2012) and older adults (Mander et al., 2015). In contrast, boosting SWA facilitated sleep-dependent memory consolidation (Marshall et al., 2006). Thus, SWA, slow oscillations in particular, is necessary and sufficient for memory consolidation during sleep. It stands to reason that slow oscillation disruptions in individuals with early AD might contribute to and accelerate the progressive memory and cognitive decline. In turn, AD pathology might further disrupt sleep-dependent brain rhythm activity that further exacerbates AD (**Figure 1**).

Mechanisms underlying slow oscillation disruptions in Alzheimer's disease

Observations from human studies demonstrated that disrupted SWA contributed to the impairments of memory consolidation in AD patients. However, the mechanisms that underlie SWA disruptions remain largely unknown. Aβ peptides target synapses and disrupt excitatory and inhibitory neurotransmission leading to neural network dysfunction

(Selkoe, 2019). This indicates that, SWA anomalies in MCI and AD patients might be due to the neuronal network dysfunction resulting from neuronal hyper- and hypoactivity. Animal studies using multiphoton microscopy elucidated deficits in inhibitory tone as one possible mechanism for disrupted SWA (Busche et al., 2008; Kastanenka et al., 2017). Deficits in synaptic inhibition led to neuronal hyperactivity (Busche et al., 2008) and caused desynchronized circuit activity within cortical excitatory neurons (Kastanenka et al., 2017). This hyperactivity was reduced when hyperactive neurons were treated with the gamma- aminobutyric acid A ($GABA_A$) agonist diazepam (Busche et al., 2008), and while slow oscillations were rescued by topical application of GABA directly onto the somatosensory cortex (Kastanenka et al., 2017). In addition to low GABA levels, the expression of $GABA_A$ and $GABA_B$ receptors was downregulated in APP mice (Kastanenka et al., 2017). Interestingly, application of either $GABA_A$ or $GABA_B$ inhibitors disrupted slow oscillations in healthy wild-type animals, mimicking slow-wave disruptions in APP mice (Kastanenka et al., 2017). As we indicated earlier, GABAergic neurons play a critical role in the onset of cortical silent states, the major element of SWA. Topical applications of a $GABA_A$ receptor agonist rescued slow waves and sleep-dependent memory consolidation in transgenic mice (Busche et al., 2015). Thus, APP mice exhibit cortical hyper- and hypoactivity due to deficits in inhibitory elements of the circuit, specifically GABA, $GABA_A$, and $GABA_B$ receptors, the activity of which is necessary and sufficient for normal SWA. AD is a truly progressive disorder. Deficits in inhibitory elements of the circuit were followed by deficits in excitatory elements (Kastanenka et al., 2019). The protein levels of the cortical excitatory neurotransmitter

glutamate were examined in APP mice. Glutamate levels were comparable in APP and wild-type littermates at 7 months of age (Kastanenka et al., 2017). However, APP mice started showing deficits in glutamate levels by 9 months of age (Kastanenka et al., 2019). Furthermore, administration of the glutamate receptor antagonists alleviated hyperactivity in APP mice (Busche et al., 2008). These findings indicate that the disturbances of synaptic inhibition followed by a deficiency in synaptic excitation within the neuronal circuits may be related to the disruptions of slow oscillations in AD.

Targeting specific GABAergic neuronal circuit elements may be particularly attractive in designing new AD therapies. Whereas restoration of parvalbumin interneuron activity acutely restored gamma oscillations (Iaccarino and Singer et al., 2016) and prevented memory loss as well as network hyperexcitability (Hijazi et al., 2020), activation of either neuronal nitric oxide synthase (nNOS) or somatostatin (SST) neurons may be useful for restoring SWA. A recent study involving the chemogenetic activation of SST- positive cells in the cerebral cortex showed increased SWA, elevated slope of individual slow waves, and prolonged NREM sleep duration compared to control conditions. Alternatively, chemogenetic inhibition of these cells reduced SWA and slow-wave incidence without changing time spent in NREM sleep (Funk et al., 2017). A previous study demonstrated that nNOS neurons are activated during episodes of NREM sleep associated with increased SWA (Gerashchenko et al., 2008). In addition, optogenetically evoked responses in nNOS-positive cells of the cerebral cortex are consistent with their role in SWS physiology (Gerashchenko et al., 2018). Furthermore, mice lacking nNOS expression in SST positive neurons exhibited significant impairments

in both homeostatic low delta frequency range SWA production and a recognition memory task that relies on cortical input (Zielinski et al., 2019). Further studies will determine whether activation of nNOS/somatostatin neurons in the cerebral cortex is efficient in reducing AD pathology, and whether this effect is mediated by SWA enhancement. Taken together, inhibition deficits followed by excitation deficits within the slow-wave circuits most likely contributed to the disruption of slow oscillations early in the disease progression and impaired sleep-dependent memory formation.

In addition to inhibitory and excitatory neurons, cortico-thalamic circuits rely on astrocytes to maintain their normal function (Araque et al., 1999; Poskanzer & Yuste, 2011, 2016). Astrocytic contributions to neuronal circuit function has been underappreciated until recently (Clarke & Barres, 2013; Kastanenka et al., 2020). Astrocytes are the glial cells that maintain glutamate and GABA recycling via glutamate/GABA-glutamine cycles. They form the tripartite synapses with pre- and post-synaptic neuronal compartments to regulate synaptic transmission via astrocytic calcium signaling (Araque et al., 1999; Newman, 2003). Furthermore, elevations in resting calcium concentrations were reported in astrocytes in APP mice (Kuchibhotla et al., 2009; Lines et al., 2022). The abnormalities in astrocytic activity may contribute to aberrant neuronal firing and lead to the disruption of neuronal networks. These results suggest that disruption of astrocytic activity may contribute to the cortico-thalamic circuit dysfunction in AD, thus perturbing SWA. Furthermore, the protein expression levels of glutamate transporter-1 (GLT-1), and glutamate aspartate transporter (GLAST), which localize specifically to astrocytic plasma membrane, were decreased in the cortex and

hippocampus in a mouse model of AD (Schallier et al., 2011). Alterations in astrocytic elements of the circuit were also reported in brain tissue from AD patients. The expression of astrocytic glutamine synthetase was decreased in close proximity to Aβ plaques in AD brains (Robinson, 2000). Interestingly, aberrant expression of glutamine synthetase was detected in a subpopulation of pyramidal neurons in AD individuals (Robinson, 2000), suggesting that the glutamate-glutamine cycle was disrupted. The abnormalities in astrocytic activity may contribute to aberrant neuronal firing and lead to the disruption of neuronal networks, thus perturbing SWA.

Astrocytes participate in triggering slow oscillation network activity

Astrocytes are traditionally known to be the supportive glial cells in the central nervous system (CNS). They are electrically silent cells that exhibit elevations in calcium transients in response to neuronal stimulation or external stimulation, such as neurotransmitters (Pasti et al., 1997). Recent studies reveal their important physiological roles including neural information processing, synaptic transmission, and neurovascular coupling (Haydon & Carmignoto, 2006), and indicate that the abnormal functions of astrocytes are associated with neurodegenerative diseases, including AD (Capani et al., 2016; Phatnani & Maniatis, 2015). Indeed, astrocytes participated in triggering slow oscillation UP states *in vitro* (Poskanzer and Yuste, 2011) and *in vivo* (Poskanzer & Yuste, 2016; Szabó et al., 2017). Electrical stimulation of individual astrocytes increases the activity of the local astrocytic networks and triggers the synchronous UP state transitions in the neighboring neurons (Poskanzer & Yuste, 2011). The authors also visualized intracellular calcium transients and demonstrated that astrocytes had

modulated extracellular glutamate, thus triggering the SWA in mouse brains (Poskanzer & Yuste, 2016). Interestingly, astrocytes exhibit calcium transients synchronized to the neuronal UP states of slow oscillations in healthy anesthetized rats (Szabó et al., 2017). In addition, more astrocytes than neurons are active during the initiation of SWA, indicating that astrocytes participate in the build-up of slow waves (Szabó et al., 2017). On the other hand, the authors showed that blocking astrocytic calcium transients resulted in reduced numbers of astrocytes and neurons participating in the SWA (Szabó et al., 2017). This series of studies supports the idea that astrocytes are necessary and play a critical role in induction of slow oscillation UP states in the cortical circuits. Therefore, understanding the role of astrocytes in the disruption of cortical SWA using animal models is important to understand the role of astrocytes in slow-wave dysfunction in AD. Finally, understanding the role of astrocytes in SWA disruptions might point to a novel therapeutic strategy for patients with AD.

Specific Aims

Slow-wave disruptions present in AD are recapitulated in mouse models of beta-amyloidosis, in which slow oscillation power is downregulated by Aβ in young APP mice (Kastanenka et al., 2017). Since slow oscillations play an important role in declarative-memory consolidation during sleep (Born, 2010; Marshall et al., 2006; Steriade & Timofeev, 2003; Walker, 2009), therapeutic targeting of slow oscillations could restore sleep and memory deficits as well as slow AD progression.

Little is known about the underlying mechanisms that cause the disruption of slow waves. Aβ initiates the impairment of slow oscillations, as Aβ targets synapses, alters

excitatory and inhibitory neurotransmission and contributes to neuronal circuit dysfunctions (Kastanenka et al., 2017; Palop & Mucke, 2010; Selkoe, 2019). Even though the causes of the slow-wave disruptions remain unknown; some suggested that the impairment in GABAergic transmission is one of the major factors (Busche et al., 2015; Kastanenka et al., 2017). As astrocytes are known to regulate the glutamate and GABA homeostasis in the synapses via glutamate/GABA-glutamine cycles; and they actively contribute to circuit function (Kastanenka et al., 2020). Therefore, astrocytes might also be one of the causes of the disruption of slow waves in APP mice. **We hypothesized that aberrant astrocytic activity contributes to the disruption of the cortico-thalamic circuit function in early stages of AD, such that restoration of astrocytic function will slow AD progression in APP mice.** To test this hypothesis, we monitored the calcium transients in individual astrocytes using high-resolution multiphoton microscopy in vivo. We discovered aberrations in astrocytic calcium signaling. Importantly, optogenetic targeting of astrocytes restored slow oscillations, decreased amyloid deposition, normalized neuronal calcium overload and rescued sleep-dependent memory function in APP mice. These results demonstrate that targeting SWA in astrocytes represent a novel therapeutic target for the prevention or treatment of AD.

The following three aims were investigated to test this hypothesis:

- Specific aim 1 (Chapter 3): To determine whether aberrant astrocytic activity is associated with slow-wave disruptions in APP mice.

- Specific aim 2 (Chapter 4): To elucidate the degree to which optogenetic stimulation of cortical astrocytes would restore neuronal slow oscillations in APP mice.
- Specific aim 3 (Chapter 5): To evaluate the degree to which optogenetic targeting of astrocytes would slow the disease progression, specifically reduce amyloid plaque deposition, normalize neuronal calcium homeostasis and rescue sleep-dependent memory function in APP mice.

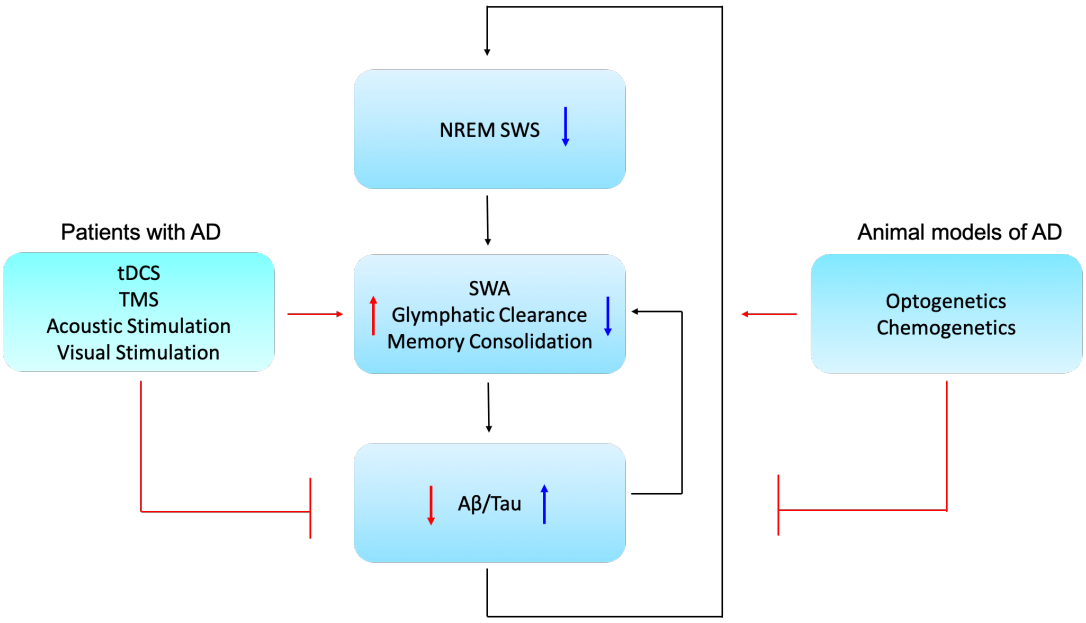

Figure 1. Schematic representation of the causal relationship between NREM SWS, memory consolidation, and AD pathology. Low NREM SWS reduced SWA and glymphatic clearance of soluble Aβ, and was associated with impaired memory consolidation. Furthermore, low SWA was associated with increased Aβ/Tau aggregation in AD patients. Proposed treatments that restore NREM SWA in AD patients and animal models of AD, provide a promising therapeutic strategy for AD.

Abbreviations: NREM SWS: Non-rapid eye movement slow-wave sleep; SWA: Slow-wave activity; Aβ: Amyloid-beta; AD: Alzheimer's disease. tDCS: Transcranial direct current stimulation; TMS: Transcranial magnetic stimulation.

CHAPTER TWO: GENERAL METHODS

Experimental animals

The mouse experiments were performed with the approval of Massachusetts General Hospital (MGH) Institutional Animal Care and Use Committees (IACUC) for the use of experimental animals. The transgenic mouse line expressing the Swedish mutation of amyloid precursor protein (APP) and deltaE9 mutation in presenilin 1 (APPswe/PS1dE9; APP mice) (Jankowsky et al., 2001) and age matched non-transgenic littermate controls (NTG) were used in the study. Age and sex of animals were specified in methods and results section for individual experiments. Mice were housed 4 animals per cage in a pathogen-free environment with ad libitum access to food and water on a 12/12 hours day and night cycle.

Stereotaxic injections

All stereotaxic injections were performed according to the following procedure. The mice were anesthetized by inhalation of 1.75% isoflurane and placed on the stereotaxic instrument with a heating pad to maintain body temperature during the injections. Eye ointment was applied to the animals' eyes prior to viral injections to prevent dryness. Fur was removed from the scalp with a trimmer. Liquid iodine was applied to the exposed skin and wiped clean with 70% isopropyl alcohol swabs 3 times each. An incision was made with sterile surgical scissors to expose the skull. A small burrhole was drilled over each injection site. Injections were performed with a 33-gauge metal needle and a 10 µl glass syringe, which was controlled by a stereotaxic injector. All the stereotaxic injections were performed at the rate of 100 nl/min. Following each

intracortical injection, the skin was sutured and animals were allowed to recover from anesthesia on a heating pad until awake and freely moving. At least four weeks were allowed for viral vector expression prior to imaging or optogenetic manipulation.

Cranial window installation and multiphoton imaging

Four weeks after yellow cameleon 3.6 (YC 3.6) viral vector injection, a cranial window was implanted over the injection site in the right somatosensory cortex of NTG and APP mice to allow monitoring of astrocytic calcium transients and neuronal calcium levels with multiphoton microscopy. To achieve this, mice were anesthetized by inhalation of 1.75% isoflurane. A round craniotomy was made with a dental drill and a 5mm glass coverslip was placed over the cortex. A mixture of dental cement and Krazy glue was used to secure the coverslip to the surrounding skull. A mode-locked titanium/sapphire laser (Mai Tai; Spectra-physics, Fremont, CA) generated two-photon fluorescence with 860 nm excitation, and three photomultiplier tubes (PMTs) (Hamamatsu Photonics, Japan) detectors collected the fluorescence emission in the range of 380-480 nm, 500-540 nm, and 560-650 nm. YC3.6-expressing astrocytes and YC3.6-expressing neuronal processes (neurites) were imaged with a 25X water immersion objective (NA=1.05, Olympus). Time-lapse images of astrocytes were acquired at a resolution of 256 x 256 pixels and sampling frequency at 2 μs/pixel. Z-stack images of neurites were acquired at a resolution of 512 x 512 pixels and a sampling frequency at 4 μs/pixel. For acquiring Z-stack images of amyloid plaques, the images were acquired with a 25X water immersion objective at a resolution of 512 x 512 pixels and a sampling frequency at 4 μs/pixel. Methoxy-XO4 (10mg/kg) was injected intraperitoneally a day

before the imaging session to detect amyloid plaques. The power of the laser was kept below 50 mW at the objective to avoid phototoxicity.

Statistics

All the statistical analyses were performed using GraphPad Prism (version 6.01). Data was reported as mean ± standard error of mean (SEM). Data sets were first tested with Shapiro-Wilk normality test, D'Agostino-Pearson omnibus normality test or Kolmogorov-Smirnov normality test. Normally distributed data was analyzed using student t test. Mann-Whitney test or Kruskal-Wallis test was used to analyze nonparametric data. *$p<0.05$ was considered significant for 2 groups.

CHAPTER THREE: ASTROCYTIC CALCIUM TRANSIENTS ASSOCIATED WITH SLOW OSCILLATIONS ARE DISRUPTED IN YOUNG APP MICE.

Introduction

Slow-wave activity disruptions in mouse models of AD

Mouse models of AD provide a powerful means to study SWA disruptions. Animal models of beta-amyloidosis recapitulate Aβ production, amyloid plaque deposition and associated neuropathology exhibited by patients with AD. In addition, animal models of tauopathy mimic tau production, intracellular tau tangles and associated neuropathology. Wide-field imaging using voltage sensitive dyes (VSD) and genetically encoded optical voltage reporters, in addition to traditional methods, such as electrophysiology, allowed monitoring SWA in mice. Similar to those in humans (Massimini et al., 2004), slow oscillations propagate across cortex in mice as traveling waves between two hemispheres (Mohajerani et al., 2010). Using VSD imaging, slow oscillation disruptions were recapitulated in young (Kastanenka et al., 2017) and older APP mice (Kastanenka et al., 2019). APP mice spent less time in NREM sleep (Roh et al., 2012). Also, their cortical slow-wave power but not the frequency was decreased (Kastanenka et al., 2017, 2019). Furthermore, Tg2576 mice exhibited decreases in SWA; and their power spectral density was shifted to higher frequencies (Kent et al., 2018). As for tauopathy models, P301S human tau transgenic mice exhibited sleep-wake cycle disruptions, reductions in NREM sleep and increased wakefulness. Moreover, their SWA was significantly decreased during NREM sleep (Holth et al., 2017). Furthermore, the transgenic mouse model 3xTg-AD, which develops plaque and tangle pathology,

exhibited slow waves at lower frequency and reduced firing rate (Castano-Prat et al., 2019). Thus, these animal models recapitulated SWA disruptions exhibited by patients with AD (Lucey et al., 2019). It should be noted that animal models do not recapitulate all aspects of the human condition. Mice have more primitive cortex and hence slow oscillations present in mice are not as complex as those recorded in humans. Despite these limitations, the mouse models were successfully used to monitor and modulate activity of specific neuronal and non-neuronal populations that contribute to the disruptions of slow waves.

Astrocytic calcium activity was altered in APP mice.

Astrocytes, similar to other neuroglia, are electrically silent in the brain. They exhibit calcium transients in response to the surrounding neuronal activity or external stimulation (Pasti et al., 1997). Furthermore, when stimulated, astrocytes are able to propagate calcium waves through gap junction to neighboring non-stimulated astrocytes inducing intercellular communication between astrocytes (Charles et al., 1991). Besides astrocyte-astrocyte communication, astrocytes were shown to regulate the activity of excitatory and inhibitory networks via propagating calcium signaling (Dani et al., 1992; Nedergaard, 1994)**.** These observations indicated that astrocytes actively participate in information processing in neural networks. Therefore, dysregulation of astrocytic intracellular calcium homeostasis may underlie the neuronal abnormalities of AD.

A study monitoring the resting calcium levels in astrocytes indicated that a percentage of astrocytes exhibited calcium elevations in APP mice regardless of their proximity to individual plaques, indicating a global response of astrocytic calcium

elevations to amyloid (Kuchibhotla et al., 2009). In addition, a recent study also demonstrated that cortical astrocytes exhibited spontaneous hyperactivity in APP mice (Backhaus et al., 2007). Elevations of calcium levels in astrocytes resulted in increased frequency of astrocytic calcium transients, independent of neuronal activity (Kuchibhotla et al., 2009; Lines et al., 2022).

Astrocytes participate in the initiation of neuronal synchronization in rodents (Szabó et al., 2017). In addition, the astrocytic calcium signaling exhibited synchrony with neuronal UP states in anesthetized rats (Szabó et al., 2017). An in vitro study showed that electrical stimulation of individual astrocytes increased the local astrocytic networks and triggered UP states of the neighboring neurons (Poskanzer & Yuste, 2011). The use of a calcium chelator inhibited the astrocytic calcium activity and significantly decreased the spontaneous and stimulated neuronal firings during UP states (Poskanzer & Yuste, 2011). This series of studies supported the idea that astrocytic calcium signaling is necessary and sufficient to induce UP states in the neuronal circuits.

These studies provided the framework for our hypothesis, which proposes that aberrant astrocytic activity contributes to the disruption of the cortico-thalamic circuit function in early stages of AD. We used a ratiometric calcium probe yellow cameleon 3.6 (YC 3.6) (Miyawaki et al., 1997), which is a fluorescence resonant energy transfer (FRET) based Ca^{2+} sensor, to determine the intracellular calcium signaling in the somas of the astrocytes in 4-6-month-old APP mice and non-transgenic controls (NTG). YC 3.6 is composed of cyan and yellow fluorescent proteins (CFP and YFP respectively) connected by a linker containing a calcium binding domain M13. When calcium is not

bound to the M13 domain, the emission intensity of CFP is high. When the structure is bound to calcium, it leads to a conformation change in the protein and brings CFP and YFP in close proximity to each other. This results in increased intensity of its FRET signal, thus increasing the emission intensity of YFP and decreasing CFP intensity. Therefore, the ratio of YFP/CFP fluorescence intensities can be calculated. In addition, the power and frequency relationships of the astrocytic calcium transients were determined using Fourier transform analysis.

Materials and Methods

Stereotaxic injection of adeno-associated viral vectors (AAVs)

Stereotaxic injections were performed as described in Chapter 2. Astrocytic calcium dynamics experiments employed 4-6-month-old APP and NTG mice. Animals were subjected to intracortical viral injections of 3 μl of AAV2/5-gfa2-YC3.6 specifically to astrocytes in right somatosensory cortex with the following coordinates: anterior–posterior (AP) -1.5 mm, lateral–medial (ML), -1.5 mm; dorsal–ventral (DV) -0.8 mm. Four weeks after YC3.6 viral vector expression, a cranial window was implanted over the YC3.6 injection site, and time-lapse imaging of astrocytes was acquired using multiphoton microscopy after cranial window implantation. The experimental procedures of cranial window installation and multiphoton imaging were described in chapter 2.

Image analysis

ImageJ was used to process the time-lapse images of YC 3.6-expressing astrocytes. YC 3.6 is a genetically encoded ratiometric calcium sensor. To determine YC3.6 ratio values, ratio images of YFP/CFP were created. Briefly, the images were

preprocessed by subtracting the background from the last image of each volume from YFP and CFP channels. A median filter with a radius of 2 was applied to each channel. The regions of interest outlining the cell body of astrocytes was manually traced and selected using ImageJ. The YC3.6 ratios of the regions of interest (ROIs) were calculated by dividing the emitted fluorescence intensity of YFP by CFP. A custom-written Matlab script was used to create the pixel-by-pixel pseudocolored images based on the YFP/CFP ratios. Fourier transform analysis was performed to determine the power and frequency relationships of the calcium transients in astrocytes. We defined the number of astrocytes cycling at slow wave frequency as the power of the astrocytic calcium transients greater than three standard deviations above the mean.

Results

Astrocytic calcium transients associated with slow oscillations are disrupted in young APP mice.

Unlike neurons, astrocytes are electrically silent and exhibit calcium transients in response to the surrounding neuronal activity or external stimulation (Pasti et al., 1997). Calcium imaging using multiphoton microscopy allows monitoring astrocytic calcium activity in vivo (Wang et al., 2014). Astrocytes actively contribute to SWA (Vaidyanathan et al., 2021), and disruptions in SWA were observed in APP mice (Kastanenka et al., 2017, 2019). Therefore, we assessed whether astrocytic calcium signaling was altered in 4-6-month-old APP mice by monitoring calcium transients within individual cortical astrocytes. We targeted YC3.6 to astrocytes in the somatosensory cortex via the astrocyte-specific glial fibrillary acidic protein (GFAP)

promoter. YC3.6 expression was visualized in the somas, processes, and endfeet of astrocytes in NTG and APP mice (Fig. 2A). The percentage of astrocytes cycling at the slow-wave frequency (0.2-1 Hz) did not differ significantly between NTG and APP mice (Fig. 2B, 72.11±3.01% of astrocytes in NTG vs 70.15±2.93% of astrocytes in APP mice; n=300 cells in 7 NTG mice, n=282 cells in 7 APP mice). APP mice exhibited aberrant calcium transients compared to NTG controls (Fig. 2C). Next, we used Fourier transform analysis to characterize the astrocytic calcium transients. The average power spectral density plots for NTG mice (n=300 cells in 7 mice) and APP mice (n= 282 cells in 7 mice) are shown in Fig. 2D. The calcium transient power, which is proportional to the square of the amplitude $[A]^2$, at the slow-wave frequency was significantly lower in young APP mice compared to that in NTG controls (Fig. 2E, 0.0080±0.00012 for NTG vs 0.0068±0.00007 for APP; ****$p<0.0001$). The frequency at peak power remained comparable in NTG and APP mice (Fig. 2F, 0.62±0.006 for NTG vs 0.63±0.016 for APP). The finding that the alterations in astrocytic calcium activity mirror those of SWA suggests an intimate role of astrocytes in slow-wave deficits.

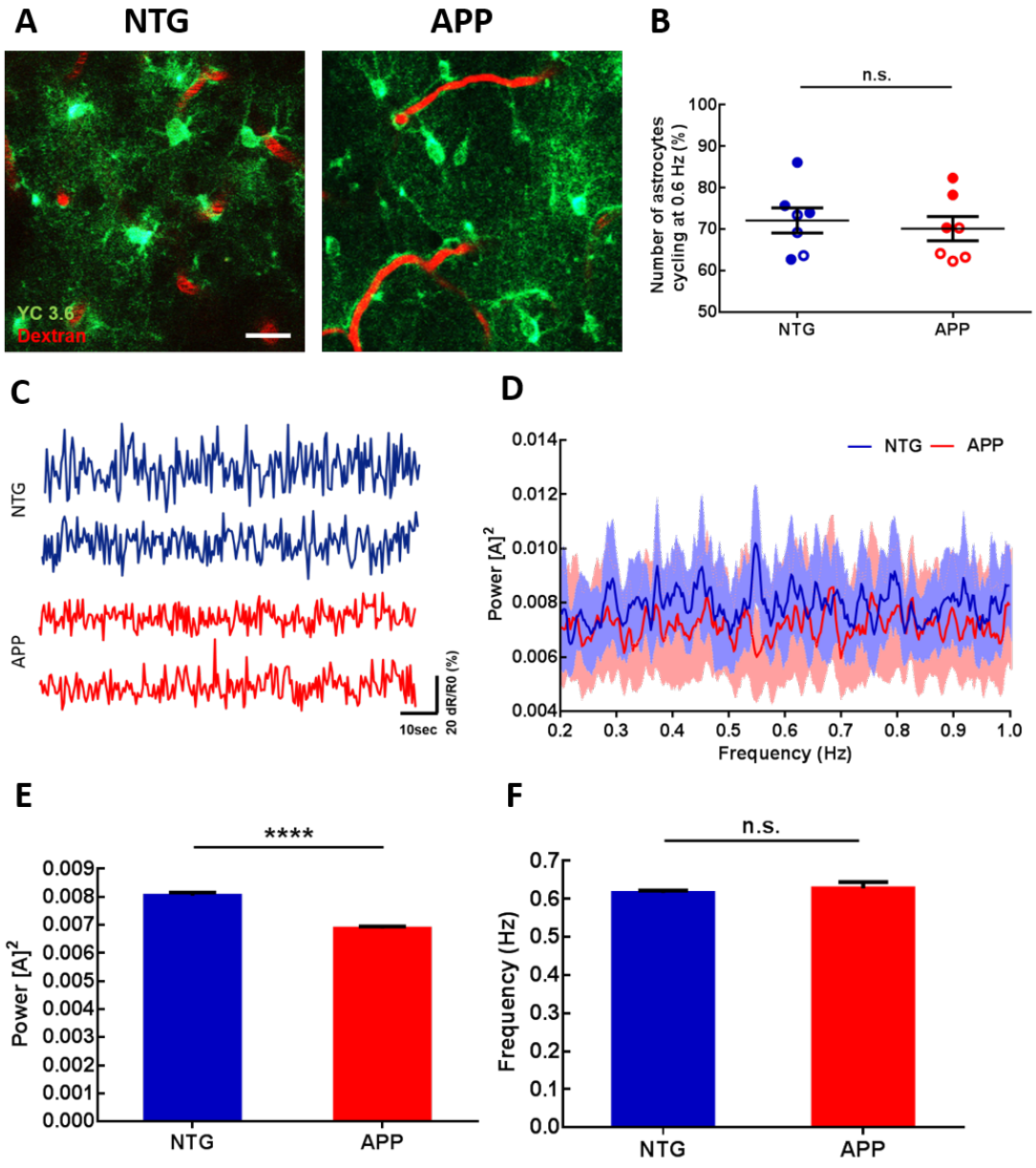

Figure 2: Astrocytic calcium transients are impaired at the slow-wave frequency in young APP mice. (A) Multiphoton microscopy image of YC3.6-expressing astrocytes in 4-6 month-old NTG and APP mice. YC3.6 was expressed in the somas, processes, and endfeet of astrocytes (green), while dextran red filled the vasculature (red). (B) The

percentage of astrocytes that exhibited calcium transients at slow-wave frequency (0.2-1 Hz) was comparable between NTG and APP groups. (C) Representative $\Delta R/R_0$ traces of individual astrocytic calcium transients in NTG and APP mice. (D) Power spectra density of astrocytic calcium transients. (E) The mean power of astrocytic calcium transients in NTG and APP mice. (F) The mean frequency of astrocytic calcium transients in NTG and in APP mice. Values are mean ± SEM, scale bar, 10μm. Males are represented by closed circles, and females by open circles. n.s non-significant, ****$p<0.0001$.

CHAPTER FOUR: OPTOGENETIC ACTIVATION OF CORTICAL ASTROCYTES RESTORES SLOW WAVES IN YOUNG APP MICE.

Introduction

To study the contribution of astrocytes to disruptions of slow oscillations, we used optogenetics to manipulate the circuit. Optogenetics is a leading-edge research tool that can be used to gain valuable insight into the causal relationship between targeted cell populations and circuit dynamics in animals (Boyden et al., 2005; Li et al., 2005). This methodology provides high spatiotemporal precision with cell-type specificity. Distinct cell types can be targeted *in vivo* using cell-type specific promoters with light-activatable channels, such as Channelrhodopsin-2 (ChR2) (Fenno et al., 2011). ChR2 is a nonspecific cationic channel that is highly permeable to protons and causes depolarization of the plasma membrane when activated by light. Light activation of cells expressing ChR2 can be used to manipulate the activity within neural circuits of interest. Optogenetics was used to increase neuronal activity in animal models of AD (Wu et al., 2016; Yamamoto et al., 2015). In addition, optogenetics was used to entrain interneurons in the gamma frequency range, restored gamma oscillations and reduced Aβ deposition in a mouse model of AD (Iaccarino et al., 2016). Our laboratory reported that light-activation of ChR2-expressing excitatory neurons at the endogenous frequency of slow waves in APP mice for 4 weeks rescued aberrant slow oscillations by restoring slow-wave power (Kastanenka et al., 2017). This resulted in halting Aβ plaque deposition and prevented intraneuronal calcium elevations (defined as calcium overload) (Kuchibhotla et al., 2008; Arbel-Ornath et al., 2017; Kastanenka et al., 2017). Alternatively, driving slow waves at

twice the endogenous frequency using optogenetics augmented Aβ production, increased neuronal calcium overload and decreased the synaptic spine density (Kastanenka et al., 2019). Besides modulating neuronal activity in mice, optogenetic manipulations of the astrocytic networks could activate astrocytes and trigger neuronal UP states in vivo (Poskanzer & Yuste, 2016). This study indicated that astrocytes can elicit slow oscillations. Thus, we performed stereotaxic injection of ChR2 specifically targeting astrocytes in left somatosensory cortex to allow activation of astrocytes with light. Next, the slow oscillations were recorded from the right somatosensory cortex, while astrocytes were optogenetically activated in the contralateral hemisphere. By doing this, we could determine whether cortical astrocytes are involved in the disruption of slow waves and whether optogenetics stimulation of astrocytes is capable to drive the cortical slow oscillations across left and right cortex in APP mice.

Materials and Methods

Stereotaxic injection of adeno-associated viral vectors (AAVs)

Stereotaxic injections were performed as described in Chapter 2. Acute optogenetics experiments used 4-6-month-old APP and NTG mice, that were injected with viral vectors targeting ChR2-mCherry or mCherry specifically to astrocytes via GFAP promoter (1.5 μl of AAV8-GFAP104-ChR2-mCherry or 1.5 μl AAV8-GFAP104-mCherry; UNC Vector Core) in the left frontal cortex (AP +1 mm, ML +1.5 mm, DV -1 mm). In addition, viral vectors encoding Cre recombinase that targeted neurons (0.75 μl AAV9-hSyn-Cre, Addgene) and Cre-dependent voltage sensor Voltron that includes a voltage-sensitive microbial rhodopsin domain Ace2N fused to a dye-capture protein

domain HaloTag (0.75 µl AAV1-hSyn-flex-Voltron-ST, Addgene) (Abdelfattah et al., 2019) were injected into the right hemispheres of the same mice (AP -3mm, ML -2mm, DV -0.2 mm) to monitor slow oscillations.

Optogenetic stimulation of ChR2-expressing astrocytes

Four weeks after ChR2-mCherry or mCherry injection in the left hemisphere and the voltage sensor Voltron injection in the right hemisphere, a synthetic fluorophore dye ligand Janelia Flour 525 dye (JF_{525} dye) (Janelia Research Campus, Ashburn, VA) (Abdelfattah et al., 2019) was injected through the retro-orbital sinus a day before the imaging to bind to the dye-capture protein domain HaloTag. JF_{525} dye was prepared by lyophilizing 100 nanomoles of JF_{525} dye and mixing in 20 µl of DMSO, 20 µl Pluronic F-127 (20% w/v in DMSO), and 100 µl of phosphate-buffered saline (PBS). On the day of imaging, NTG and APP mice underwent cranial window installation to allow recording of slow oscillations in the right hemisphere. A 5mm glass coverslip was placed over the right hemisphere. After the cranial window surgery, a fiber-optic cannula (length=2mm, Doric Lenses Inc, Quebec, Canada) was implanted over the ChR2-mCherry or mCherry injection site to activate astrocytes. Cannula tip was positioned above the cortex to prevent penetration and disruption of cortical circuit activity. The cannula and glass coverslip were secured with the dental cement mixture to the surrounding skull. The activity of neurons expressing Voltron labeled with JF_{525} was recorded with an upright fluorescence microscope with 2X objective (NA=0.14, Olympus). An mKO/mOrange filter set (excitation: 530/30 nm, emission: 575/40 nm), and a 550LP dichroic mirror (49014, Chroma Technology, Bellows Falls, VT) were used for fluorescence imaging of

Voltron and JF_{525} expression. A complementary metal oxide semiconductor (CMOS) camera (Hamamatsu Photonics, Japan) was used to collect images at 20 Hz. 3-5 trials of spontaneous slow oscillations were collected in the absence of optogenetic stimulation. Following these acquisitions, a fiber-optic patch cord (Doric Lenses Inc, Quebec, Canada) was attached to the cannula to activate ChR2-expressing astrocytes in left frontal cortex. 400 ms pulses of 473 nm light (3-6 mW) generated by a diode laser (Optoengine, Midvale, UT) were applied to the cortex at 0.6 Hz in APP mice and 1.2 Hz in NTG mice while recording slow oscillations. Replicates of 3-5 trials were acquired.

Immunohistochemistry

The mice that underwent acute optogenetic stimulation expressing either ChR2-mCherry or mCherry empty vector specifically targeted to astrocytes were processed for immunohistochemistry as follows. The animals were euthanized with carbon dioxide inhalation and perfused transcardially with 1X PBS. The left hemisphere that was injected with ChR2-mCherry or mCherry was harvested and fixed in 4% paraformaldehyde for 24 hours, then the brain was cryoprotected by 30% glycerol in 1X PBS. For visualizing viral infusion, the brain was cryosectioned into twenty-micrometer coronal sections, which were subjected to antigen retrieval in citrate buffer. Then the sections were permeabilized with Triton X-100. Normal goat serum (NGS) was used to block non-specific antibody binding in tissues. The following primary antibodies that specifically targeted neuronal nuclei (NeuN; mouse monoclonal anti-NeuN, 1:500, MAB377; Millipore Sigma), glial fibrillary acidic protein (GFAP; rabbit polyclonal anti-GFAP, 1:1000; abcam ab7260), or ionized calcium binding adaptor molecule 1 (Iba-1;

rabbit monoclonal anti-Iba1, 1:200; abcam ab178846) were used in the study. The sections were incubated with primary antibodies at 4°C overnight. Then the sections were incubated with the secondary antibodies, anti-mouse-pacific blue 405 (1:250) and/or anti-rabbit-Alexa fluor 488 (1:1000), for 1 hour at room temperature. The sections were mounted with mounting media (Vectashield Antifade, Vector Laboratories) either with or without DAPI (4',6-diamidino-2-phenylindole). Sections were examined using an inverted Zeiss microscope with 10X objective. ROIs were selected in cortex. NeuN, GFAP, and Iba-1 expressing cells were manually identified using ImageJ. The percentage of GFAP-positive cells that colocalize with mCherry-positive cells were calculated. Also, the percentage of NeuN and Iba-1-negative mCherry-positive cells were calculated and presented in the figures.

Image analysis

The time-lapse images of cortical slow oscillations that were acquired with the CMOS camera were analyzed using ImageJ. The fluorescence intensity from Voltron_JF_{525} images were measured as the change in the pixel intensity over the baseline ($\Delta F/F_0$). Fourier transform analysis was used to quantify the $\Delta F/F_0$ traces of Voltron_JF_{525} images to determine the power of slow oscillations at 0.4-0.6 Hz, and the power of slow oscillations at 1.2 Hz when astrocytes were optogenetically activated at twice the endogenous frequency of slow oscillations.

Results

Optogenetic activation of cortical astrocytes restores slow waves in young APP mice.

The power of slow waves is significantly lower in APP mice compared to NTG mice at 3-6 months of age, while the frequency remains comparable at 0.6 Hz (Kastanenka et al., 2017). Since astrocytes actively contribute to slow oscillations and astrocytic calcium transients associated with slow waves are disrupted, we tested whether optogenetic activation of astrocytes would restore neuronal slow oscillations in APP mice.

To verify that ChR2-mCherry and mCherry targeted astrocytes and no other brain cells, we performed immunohistochemical analyses of the localization of mCherry with neuronal (NeuN), astrocytic (GFAP), and microglial (Iba1) markers in post-mortem brain tissue (Fig. 3B, C, I). mCherry-expressing cells colocalized with GFAP+ positive cells (Fig. 3E; 92.74±1.21% of cells GFAP+; 825/891 cells from 10 sections in 5 mice), not NeuN (Fig. 3F; 98.43±0.47% cells NeuN-; 877/891 cells from 10 sections in 5 mice) or Iba1 (Fig. 3K; 98.24±0.52% of mCherry-expressing cells lacked Iba-1; 421/431 cells from 10 sections in 6 mice). Thus, the GFAP promoter targeted ChR2-mCherry or mCherry alone specifically to astrocytes, not neurons or microglia.

3-5-month-old APP and NTG mice received viral delivery of ChR2 or mCherry lacking ChR2. Viral vectors targeted astrocytes via the GFAP promoter in the left hemisphere (Fig. 4A). In addition to ChR2 or mCherry injections in the left hemisphere, animals received viral injections of a voltage sensor Voltron and AAV9-hsyn-Cre into the contralateral somatosensory cortex (Fig. 4A). Subsequently, a cannula was implanted over the ChR2/mCherry injection site and a 5mm cranial window was installed over the right somatosensory cortex expressing Voltron (Fig. 4B, C). Cortical slow waves were

monitored using wide-field microscopy, before and during light activation of ChR2/mCherry-expressing astrocytes (Fig. 4D-F).

Neuronal population imaging using Voltron revealed disruptions of slow oscillations in APP mice, consistent with earlier reports (Fig. 4D) (Kastanenka et al., 2017). To determine whether optogenetic targeting of astrocytes was able to drive slow oscillations, we stimulated astrocytes at twice the endogenous frequency of slow waves, 1.2Hz, in NTG mice. This allowed us to distinguish between endogenous slow oscillations and optogenetically elicited slow waves. Optogenetic targeting of astrocytes elicited slow waves at twice the endogenous frequency (Fig. 4E Spon v.s. ChR2 2XRx). However, light stimulation of mCherry in absence of ChR2 failed to do so (Fig. 4E Spon v.s. mCherry 2XRx). Furthermore, light activation of ChR2-expressing astrocytes at the endogenous frequency of slow waves, 0.6Hz, restored the SWA in APP mice (Fig. 4F Spon v.s. ChR2 1XRx). Yet, light activation of mCherry in absence of ChR2 failed to do so (Fig. 4F Spon v.s. mCherry 1XRx).

Fourier transform analysis was performed to elucidate the power-frequency relationships. The power spectral densities of slow oscillations were plotted using Matlab (Fig. 4G-I). Endogenous slow waves oscillated spontaneously at 0.4-0.6 Hz in NTG and APP mice (Fig. 4G) (Kastanenka et al., 2017). Fourier transform analysis revealed decreases in the power of spontaneous slow waves in APP mice compared to NTG group (Fig. 4G, J; n=37 traces in 6 NTG mice, n=30 traces in 6 APP mice). The slow-wave power was significantly lower in young APP mice (Fig. 4J; $1.27x10^{-6}\pm3.54x10^{-7}$ for NTG vs $1.93x10^{-7}\pm6.48x10^{-8}$ for APP; ***$p<0.001$). A spectral power density plot revealed a

pronounced peak at 1.2 Hz in NTG mice whose astrocytes were optogenetically driven at 1.2 Hz (ChR2 2XRx), but not in mCherry-expressing (mCherry 2XRx) controls (Fig. 4H, red box). The power at 1.2 Hz increased significantly during optogenetic stimulation, but not light stimulation of mCherry (Fig. 4K; $5.19x10^{-8}\pm7.45x10^{-9}$ for Spon vs $1.29x10^{-7}\pm2.56x10^{-8}$ for mCherry 2XRx vs $1.17x10^{-6}\pm1.28x10^{-7}$ for ChR2 2XRx; ****$p<0.0001$) (Fig. 4H, K; NTG Spontaneous: n=37 traces in 6 mice, NTG mCherry 2XRx: n=61 traces in 5 mice, NTG ChR2 2XRx: n=40 traces in 5 mice). This suggested that optogenetic stimulation of cortical astrocytes was able to drive SWA at twice the endogenous frequency in NTG mice.

We then determined whether optogenetic targeting of astrocytes restored slow oscillation power in APP mice. Optogenetic stimulation of ChR2-expressing astrocytes at the endogenous frequency of slow waves, 0.6Hz, restored the power of slow waves in APP mice (Fig. 4I, red box, L; $1.93x10^{-7}\pm6.48x10^{-8}$ for Spon vs $2.56x10^{-7}\pm4.07x10^{-8}$ for mCherry 1XRx vs $5.82x10^{-7}\pm9.63x10^{-8}$ for ChR2 1XRx; **$p<0.01$; ****$p<0.0001$) (Fig. 4I, L; APP Spontaneous: n=30 traces in 6 mice, APP mCherry 1XRx: n=45 traces in 5 mice, APP ChR2 1XRx: n=53 traces in 5 mice). Thus, the SWA was restored following light activation of astrocytes at the endogenous frequency of slow waves. These results indicated that optogenetic targeting of astrocytes could be used to successfully manipulate neuronal slow oscillations in APP mice.

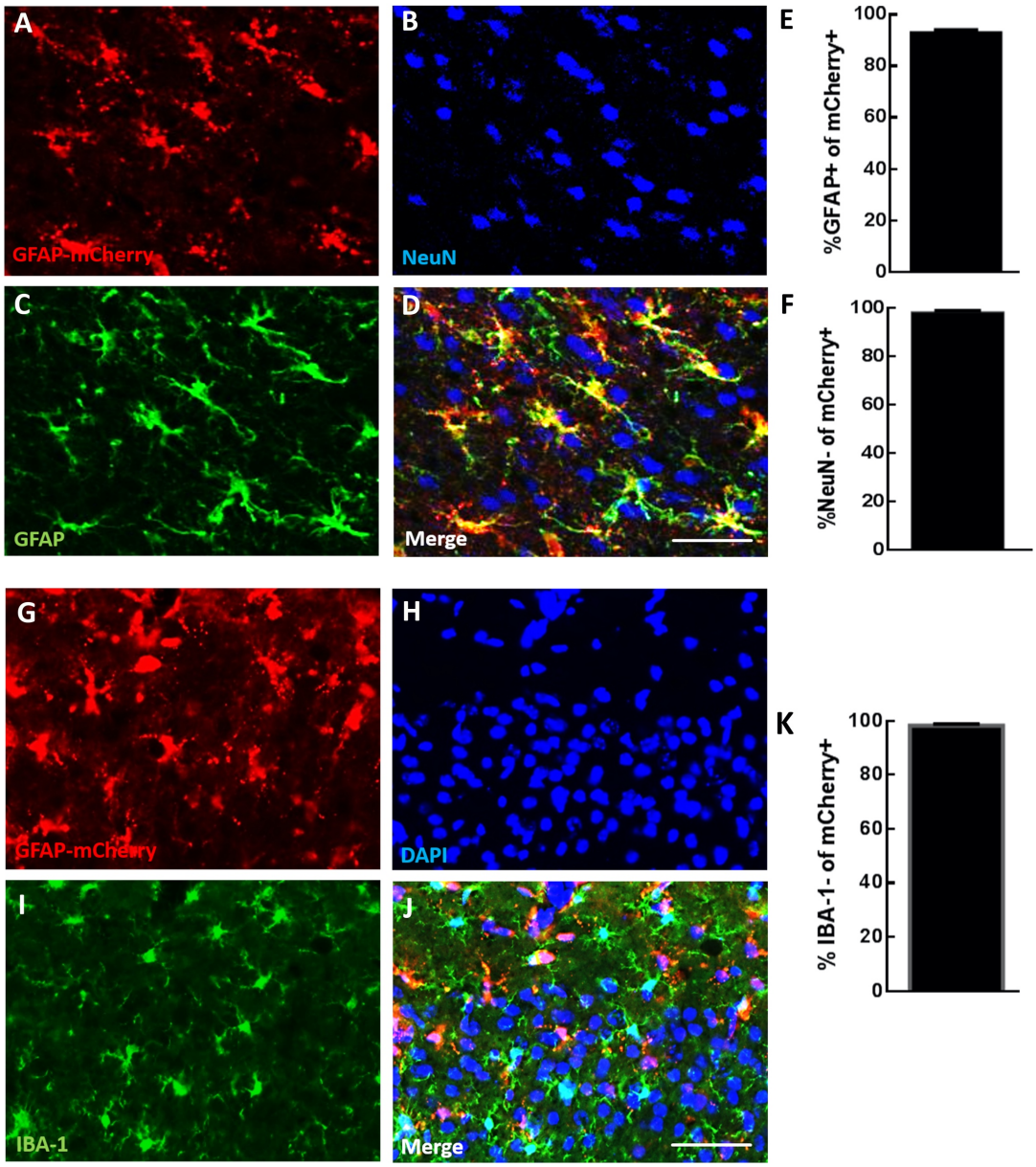

Figure 3: GFAP promoter targets cortical astrocytes with high fidelity, not neurons or microglia. (A, G) Representative images showing GFAP-mCherry expression in cortical astrocytes. (B, C) neuronal nuclei (NeuN) (B) and glial fibrillary acidic protein (GFAP) (C) expression following Immunohistochemical staining. (D) Merge image A-C.

(E, F) GFAP-mCherry was expressed in >92% of GFAP-expressing astrocytes. GFAP-mCherry-labeled astrocytes were mostly NeuN-. (H, I) DAPI-labeled cells and microglia marker Iba-1 expression following immunohistochemical staining. (J) Merge image G-I. (K) GFAP-mCherry-labeled astrocytes were mostly IBA-1-. Values are mean ± SEM, Scale bar, 50μm.

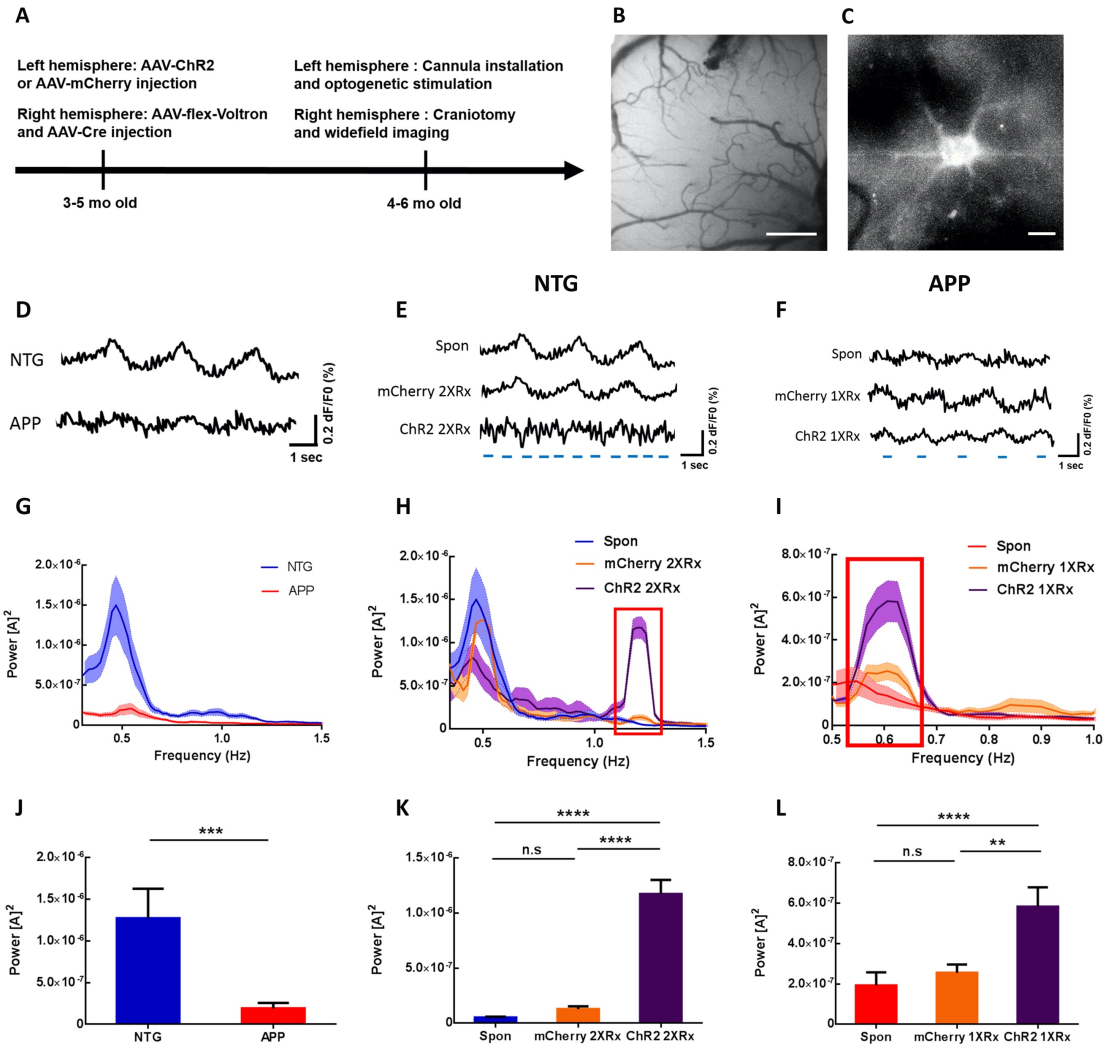

Figure 4: Optogenetic targeting of astrocytes allows manipulation of slow oscillations. (A) Experimental design. (B) Low resolution wide-field image of Voltron fluorescence. Scale bar, 500µm. (C) High resolution wide-field image of a neuron expressing Voltron. Scale bar, 10µm. (D) Representative traces of voltage sensor signal in NTG and APP mice. (E) Representative traces of voltage sensor signal acquired spontaneously (Spon), during light activation of mCherry lacking ChR2 at 1.2 Hz

(mCherry 2XRx), or during optogenetic activation of ChR2 at 1.2 Hz (ChR2 2XRx) in NTG mice. Light pulse stimulations are shown in blue. (F) Representative traces of voltage sensor signal acquired spontaneously (Spon), during light activation of mCherry lacking ChR2 at 0.6 Hz (mCherry 1XRx), or during optogenetic activation of ChR2 at 0.6 Hz (ChR2 1XRx) in APP mice. Light pulse stimulations are shown in blue. (G, H, I) Power spectral density plots of slow oscillations in NTG and APP mice across conditions. (J) Bar graph comparing the average power of slow oscillations in NTG and APP mice. (K) Bar graph comparing the average power of slow oscillations in NTG mice across conditions. (L) Bar graph comparing the average power of slow oscillations in APP mice across conditions. **$p<0.01$, ***$p<0.001$, ****$p<0.0001$.

CHAPTER FIVE: RESTORATION OF SLOW OSCILLATIONS THROUGH OPTOGENETIC TARGETING OF CORTICAL ASTROCYTES REDUCES AMYLOID DEPOSITION, NORMALIZES NEURONAL CALCIUM OVERLOAD, AND IMPROVES SLEEP-DEPENDENT MEMORY PERFORMANCE IN APP MICE.

Introduction

YC3.6 utility as a functional readout of treatment efficacy in mouse models of Alzheimer's disease

Calcium ions play a critical role in regulating a myriad of cellular and specifically neuronal functions including but not limited to neurotransmission, synaptic activity, as well as the processes of learning and memory (Berridge, 1998, 2014). Disruptions in calcium homeostasis have been observed in a variety of neurodegenerative diseases, including Alzheimer's disease (AD) (Berridge, 2011; Bezprozvanny & Mattson, 2008; Green & LaFerla, 2008; Henstridge et al., 2019). The calcium hypothesis of AD was coined by Zaven Khachaturian and has been widely accepted since (Khachaturian, 1994). Elevations in basal calcium levels have been reported in neurons, glial cells and cellular compartments, such as mitochondria (Calvo-Rodriguez et al., 2020; Kastanenka et al., 2016; Kuchibhotla et al., 2008, 2009; Lines et al., 2022). Therefore, a better understanding of how calcium homeostasis contributes to AD will allow development of novel therapeutic approaches to slow the disease progression.

Calcium imaging is a powerful tool used to monitor calcium activity *in vivo* using high resolution multiphoton microscopy (Stosiek et al., 2003). Differential approaches of

targeting the genetically encoded calcium indicators to specific cell types or cellular compartments have been developed, such as the ratiometric calcium sensor, YC3.6 and the calcium indicators based on a single fluorescent protein GCaMPs (Miyawaki et al., 1997; Nagai et al., 2004; Nakai et al., 2001; Persechini et al., 1997; Romoser et al., 1997; Whitaker, 2010). These approaches allowed visualization of calcium within distinct cells and cellular compartments.

The ratiometric calcium sensor, YC3.6, is a genetically encoded calcium indicator based on FRET. It allows quantitative measurements of intracellular calcium concentrations in individual neuronal and non-neuronal cells as well as distinct cellular organelles (Miyawaki et al., 1997; Nagai et al., 2004). YC3.6 is the brightest calcium indicator within the YC family. It exhibits the largest dynamic range and an improved signal-to-noise ratio enabling *in vivo* calcium imaging in the brains of living, breathing mice (Nagai et al., 2004). YC3.6 is composed of a CFP and YFP that serve as donor and acceptor respectively for FRET. It also contains calmodulin, and calmodulin-binding domain M13. Binding of calcium to calmodulin initiates a conformation change in calmodulin and M13, which brings CFP and YFP in closer proximity to each other (Miyawaki et al., 1997; Nagai et al., 2004). This results in increased intensity of the FRET signal, so that the emission wavelengths of both the donor and the acceptor can be measured.

YC3.6 use has a number of advantages and disadvantages compared to the use of other genetically encoded calcium indicators based on a single fluorescent protein, such as GCaMPs (T.-W. Chen et al., 2013; Dana et al., 2019; Nakai et al., 2001). The

advantage of using ratiometric sensors, such as YC 3.6, is the ratio of YFP to CFP fluorescence intensities can be converted directly to a quantitative calcium measure. Thus YC3.6 allows determination of the absolute calcium concentration within cells and cellular compartments. This is not possible using single wavelength reporters like GCaMPs as it is impossible to distinguish between the level of expression of the probe with the calcium concentration (Whitaker, 2010). The disadvantage of using YC3.6 is its inferior signal-to-noise ratio compared to GCaMPs, and slower kinetics, but is still able to report calcium dynamics. GCaMPs are based on a single fluorescent protein and are better able to detect the dynamic changes in intracellular calcium levels (Nakai et al., 2001). Thus, GCaMPs are better suited to measure the relative calcium changes within cells and cellular compartments (Whitaker, 2010).

Multiphoton imaging is a high-resolution imaging technology that allows imaging of structure and function within intact mouse brains. Thus, it allows imaging at the cellular and subcellular levels. It provides high spatial (up to 1 micron) and temporal (up to 30Hz) resolutions and has been extensively used in studying neuropathological features as part of Alzheimer's progression using transgenic mouse models of AD (Wang et al., 2014). The use of YC3.6 provides an attractive methodology for visualizing basal calcium changes as part of disease progression or a treatment regimen. Since YC3.6 is a genetically encoded calcium indicator, it can be stably expressed in targeted neuronal or non-neuronal cells *in vivo* for 6 months or longer after viral delivery of YC3.6 to cells of interest via cell-specific promoters (Arbel-Ornath et al., 2017; Kastanenka et al., 2016; Kuchibhotla et al., 2008). This allows repeated visualization of YC3.6 in the same

neuronal or non-neuronal cells with repeated imaging using multiphoton microscopy. Thus, absolute changes in basal calcium levels can be determined with repeated measure analyses.

Transgenic mouse models of beta-amyloidosis, such as APP and Tg2576 mice, exhibit a small yet vulnerable cortical neuronal population with elevations in basal intracellular calcium, termed calcium overload (Kuchibhotla et al., 2009; Kastanenka et al., 2016; Lines et al., 2022). Neuronal calcium elevations are evident early in the disease progression around the time of cortical amyloid deposition at 5 months of age in APP mice and increase in the course of the disease progression amounting up to ~20% of neuronal processes exhibiting calcium overload (Kuchibhotla et al., 2008). Neuronal processes in close proximity to amyloid plaques were more vulnerable to calcium dyshomeostasis and exhibited greater incidence of calcium overload (Kuchibhotla et al., 2008). Moreover, neuronal calcium overload also altered the morphology of individual neurons and disrupted the compartmentalization of calcium in dendritic spines (Kuchibhotla et al., 2008). Soluble amyloid-β was responsible for the neuronal calcium elevations, since application of transgenic conditioned media (TgCM) or amyloid-beta derived diffusible ligands (ADDLs) enriched with soluble amyloid-β oligomers (AβOs) directly to neurons, increased resting intracellular calcium levels in those neurons (Arbel-Ornath et al., 2017; Wang et al., 2018) and resulted in loss of dendritic spines or synapses within 24 hours of treatment (Arbel-Ornath et al., 2017).

Since neuronal calcium levels are elevated in animal models of amyloidosis, restoration of neuronal calcium levels can serve as a functional readout of treatment

efficacy. The therapeutic effect of chronic treatment with an amyloid-β immunotherapy aducanumab was evaluated using calcium imaging in adult Tg2576 mice, which overexpress amyloid precursor protein with the Swedish mutation and start depositing amyloid-β plaques at 13 months (Kastanenka et al., 2016). Anti-amyloid immunotherapies showed great promise in mouse models of AD (Bouter et al., 2015; Sevigny et al., 2016). Neuronal calcium levels were monitored in YC3.6-expressing cortical neurons prior to antibody treatment and in the course of treatment with 10mg/kg administration of aducanumab for the period of 6 months. Prior to antibody treatment, Tg2576 mice exhibited significant calcium elevations, calcium overload, in their cortical neurons. Remarkably, weekly systemic treatment with aducanumab decreased the number of neurons with calcium overload in the course of treatment and restored neuronal calcium levels to control levels (Kastanenka et al., 2016). Aducanumab was recently approved by FDA as Aduhelm as the first disease-modifying therapy for AD. Additionally, the therapeutic efficacy of monoclonal antibody ACU3B3, targeting AβOs specifically, was tested in adult non-transgenic mice challenged with AβOs (Wang et al., 2018). Calcium imaging revealed that the intracellular calcium level in YC3.6-expressing neurons was significantly increased after brain exposure to AβOs. These calcium elevations were prevented by pre-treatment of the brains with 1ng/ml ACU3B3 (Wang et al., 2018).

Also, the therapeutic potential of a novel multimodal botanical drug, NB-02 (earlier known as DA-9803) was tested using YC3.6 *in vivo* (Lee et al., 2021; Pagnier et al., 2018). These studies implemented APP mice that also exhibit calcium overload in

cortical neurons. The first study tested the potential of NB-02 to prevent AD pathophysiology in young APP mice. Oral gavage with NB-02 prevented calcium elevations in cortical neurons of young APP mice (Pagnier et al., 2018). Subsequently, NB-02's potential was tested as treatment in old APP mice. To that end the effect of NB-02 on restoring neuronal calcium levels was determined. Old APP mice exhibit extensive calcium overload within their cortical neurons. Gavage treatment with the botanical drug normalized calcium homeostasis and restored basal calcium to control levels in APP mice (Lee et al., 2021). Therefore, these studies showed that NB-02 holds promise as a preventative or therapeutic agent for AD.

Finally, the effect of brain rhythm manipulation was determined on Alzheimer's progression using multiphoton imaging of YC3.6-labelled neurons. Optogenetic restoration of SWA in APP mice at the endogenous frequency prevented neuronal calcium overload, thus slowing disease progression in APP mice (Kastanenka et al., 2017). On the other hand, optogenetic increases in SWA increased the number of neurons with calcium overload, thus facilitating disease progression in APP mice (Kastanenka et al., 2019).

Thus, YC3.6 has been successfully utilized as a functional indicator of treatment efficacy in a variety of mouse models of AD. It provided useful insights into the neuronal function during AD progression and in the course of treatment regimens. Thus, restoration of calcium homeostasis should be pursued as a potential therapeutic strategy to reverse AD pathology or prevent it altogether.

Optogenetics alteration of neuronal circuits improves memory performance in mice.

Optogenetic modulation of brain wave activity restored memory deficits in experimental models. Synchronization of SWA in somatosensory and motor cortices using optogenetics was able to restore perceptual memory impairment and prolong memory retention in sleep-deprived mice (Miyamoto et al., 2016). In addition, restoration of hippocampal oscillations with optogenetics resulted in an improvement of recognition memory in APP mice (Giovannetti et al., 2018). Also, optogenetic activation of memory engram cells in hippocampus increased spine density in engram cells and restored long-term memory (Roy et al., 2016). Furthermore, gamma oscillation rescue using optogenetics improved spatial memory in an AD mouse model (Etter et al., 2019). Restoring brain oscillations by optogenetic approaches in mouse models provides insight into novel therapeutic approaches to treat and/or prevent AD altogether. Animal studies suggest that restoring brain oscillation activity, including SWA, may be an effective therapeutic strategy for reducing memory deficits in AD patients.

Materials and Methods

Stereotaxic injection of adeno-associated viral vectors (AAVs)

Stereotaxic injections were performed as described in Chapter 2. Chronic optogenetic experiments employed 8-10-month-old APP mice, that received stereotaxic injections of 1.5 µl of AAV8-GFAP104-ChR2-mCherry or 1.5 µl AAV8-GFAP104-mCherry into left frontal cortices (AP +1 mm, ML +1 mm, DV -1 mm). Furthermore, 3 µl of AAV2-CBA-YC3.6 was injected into right somatosensory cortices (AP -2 mm, ML

-1.5 mm, DV -1 mm) of same mice to allow monitoring neuronal calcium dynamics with multiphoton microscopy. 400 ms pulses of 473 nm light (5-10 mW) were delivered at 0.6 Hz, 24 hr/day for 14 or 28 days to restore the power of slow oscillations in the APP mice. Mice were housed in microdialysis bowls (Harvard Apparatus, Holliston, MA) with free access to food and water during entire optogenetic treatment. Following the chronic light treatment, mice were subjected to open field and fear conditioning tests. Mice were handled 3 days before treatment. Then the mice were subjected to multiphoton imaging of amyloid plaques and YC3.6-expressing neurons as described in Chapter 2.

Open field and contextual fear conditioning tests

Another cohort of NTG and APP mice expressing ChR2-mCherry or mCherry were subjected to open field and fear conditioning tests after receiving optogenetic treatment. Mice were handled 3 days before treatment. Following 13 days of chronic light treatment, the fiber-optic patch cords were removed from the mice to conduct the open field and fear conditioning tests. Mice were placed in a 27 cm x 27 cm x 27 cm arena one at a time and allowed to move freely for 10 mins in a dark room during open field test. A camera recorded the locomotor activity of mice, and EthoVision XT software (Noldus, Wageningen, the Netherlands) was used to track and analyze the locomotor activity of APP mice.

Following the open field test, mice were placed in fear conditioning chambers (30 × 24 × 21 cm; MED-Associates, St. Albans, VT) one at a time and were monitored with a video camera for 5 minutes. Mice received 3 foot-shocks (1 s, 0.6 mA, 1 minute interval) after 2 minutes of baseline recording. The conditioning chambers were surrounded with

aluminum sides and a clear polycarbonate door. The foot-shocks were delivered with a removable grid floor that contained 36 stainless steel grid rods (3.18 mm in diameter, 8.13 mm apart). Following fear acquisition, mice were returned to the microdialysis bowls, their cannulas were connected to the fiber-optic patch cords for the last day of chronic light treatment. The day after fear acquisition, all mice were returned to the conditioning chambers for fear recall (recording for 3 minutes) in absence of foot-shocks. The threshold of freezing levels (i.e., the value of the motion index below which no movement is detectable) was determined. Fear responses measured as percentage of time spent freezing were determined using Video Freeze software (Med associates Inc, Fairfax, VT).

Image analysis

Amyloid plaque image analysis was performed as follows. First, maximum intensity projections of each Z-stack volume were generated with Matlab. Then, ImageJ was used to manually select the ROIs for each plaque. Lastly, amyloid plaque number and amyloid plaque burden were counted and measured with the custom-written Matlab script. Data were presented as amyloid plaque numbers per cortical volume. Alternatively, amyloid plaque burden was calculated as percentage of cortical area occupied by amyloid. The z values of Z-stacks were comparable across conditions.

ImageJ was used to process the Z-stack images of YC 3.6-expressing neurites. YC 3.6 is a genetically encoded ratiometric calcium sensor. To determine YC3.6 ratio values, ratio images of YFP/CFP were created. Briefly, the images were preprocessed by subtracting the background from the last image of each volume from YFP and CFP

channels. A median filter with a radius of 2 was applied to each channel. The regions of interest neurites were manually traced and selected using ImageJ. The YC3.6 ratios of ROIs were calculated by dividing the emitted fluorescence intensity of YFP by CFP. A custom-written Matlab script was used to create the pixel-by-pixel pseudocolored images based on the YFP/CFP ratios.

Results

The rhythmic optogenetic stimulation of astrocytes decreases amyloid beta deposition.

Since optogenetic targeting of astrocytes restored slow waves, and SWA actively contributes to the clearance of Aβ (Xie et al., 2013), we sought to determine whether astrocytic targeting using optogenetics could slow the accumulation of Aβ in APP mice. To that end, ChR2- or mCherry-expressing cortical astrocytes were stimulated with light at 0.6 Hz, 24 hours per day continuously for 2 or 4 weeks in aged APP mice. At the end of the light treatment, cranial windows were installed over the right posterior cortex, contralateral to the ChR2/mCherry site. High-resolution multiphoton microscopy allowed monitoring of methoxy-X04-positive amyloid plaques after treatment *in vivo* (Fig. 5A). Multiphoton images revealed the presence of amyloid plaques in 8-10-month-old APP mice (Fig. 5B, C). Restoring slow oscillations decreased amyloid deposition in the ChR2 group (Fig. 5C) as compared to mCherry controls (Fig. 5B). Amyloid plaque burden, which takes into account plaque numbers and size, was significantly lower after optogenetic treatment compared to light activation of mCherry (Fig. 5D; 1.43±0.11 % burden for mCherry vs 1.01±0.06 % burden for ChR2; mCherry: n=57 fields of view

(FOV) in 8 APP mice; ChR2: n=82 FOV in 10 APP mice; **P<0.01). Also, the number of amyloid plaques was significantly lower in the ChR2 group compared to that in mCherry controls (Fig. 5E; 185.9±14.44 plaques/mm^3 for mCherry vs 139.0±5.69 plaques/mm^3 for ChR2; mCherry: n=57 FOV in 8 APP mice; ChR2: n=82 FOV in 10 APP mice; *P<0.05). Therefore, astrocyte-dependent rescue of slow waves reduced the rate of amyloid plaque deposition in APP mice.

The rhythmic optogenetic stimulation in astrocytes normalizes neuronal calcium levels in APP mice.

Intracellular calcium ions are necessary for healthy neuronal function and are tightly regulated through calcium homeostasis. APP mice exhibit disruptions in neuronal calcium homeostasis that results in elevated resting calcium levels, or calcium overload (Arbel-Ornath et al., 2017; Kuchibhotla et al., 2008). Calcium levels were monitored using multiphoton microscopy. A genetically encoded ratiometric calcium reporter YC3.6 under the chicken ß–actin promoter (CBA) promoter was used to target cortical neurons. YC3.6 allows for determination of basal calcium levels in neurons. We determined whether light activation of ChR2-expressing astrocytes would alter neuronal calcium levels in APP mice. Thus, neuronal calcium was used as a functional readout of treatment efficacy. The majority of neuronal processes exhibited normal calcium levels in APP mice (Fig. 6A blue neurons). However, these animals also exhibited neurons with calcium overload (Fig. 6A red neuron, white arrows). Restoration of slow waves led to a decrease in the percentage of neurons with calcium overload (Fig. 6B). A YC3.6 ratio greater than two standard deviations above the mean value (>1.73) in NTG neurons was

defined as calcium overload (Fig. 6C red box) (Kastanenka et al., 2019). The percentage of neuronal processes exhibiting calcium overload was lower in the ChR2 group compared to the mCherry group (Fig. 6C, D; 12.65±1.8% for mCherry vs 5.79±1.2% for ChR2; mCherry: n=2182 neurites in 23 FOV of 7 mice; ChR2: n=2014 neurites in 24 FOV of 6 mice; *$p<0.05$). Thus, astrocyte-dependent rescue of slow waves decreased neuronal calcium overload and restored neuronal calcium homeostasis in APP mice.

The rhythmic optogenetic stimulation in astrocytes improves sleep-dependent memory performance in APP mice.

To determine whether optogenetic targeting of astrocytes enhanced memory consolidation, we tested long-term memory using contextual fear conditioning in NTG controls and APP mice (Fig. 7A). Fear acquisition was performed on day 13 of light treatment. The freezing levels at baseline were similar in all three groups (Fig. 7B; 2.44±1.13% for NTG mCherry vs 2.77±0.79% for APP mCherry vs 2.90±0.77% for APP ChR2). Delivery of 3 consecutive electric shocks resulted in progressive increases in freezing. Additionally, the freezing levels after the delivery of first, second and third shocks were comparable between respective mCherry and ChR2 groups (Fig. 7B; 1^{st} shock: 18.17±10.7% for NTG mCherry vs 12.04±5.93% for APP mCherry vs 9.97±4.13% for APP ChR2; 2^{nd} shock: 38.04±7.81% for NTG mCherry vs 15.25±6.48% for APP mCherry vs 31.52±6.41% for APP ChR2; 3^{rd} shock: 46.23±9.54% for NTG mCherry vs 27.82±9.49% for APP mCherry vs 33.12±7.32% for APP ChR2). Thus, fear acquisition was not altered significantly by optogenetic treatment of APP mice. Following fear acquisition, the mice were allowed to consolidate their memories

overnight during light activation of ChR2 or mCherry. Fear recall was tested the following day. The contextual fear memory was impaired in APP mice (Fig. 7C; 87.29±1.67% for NTG mCherry vs 65.73±4.92% for APP mCherry; **$p<0.01$). The freezing levels were significantly higher in APP ChR2 group compared to that in APP mCherry group (Fig. 7C; 65.73±4.92% for APP mCherry vs 82.46±6.73% for APP ChR2; *$p<0.05$). In addition, the freezing levels were comparable between NTG mCherry group and APP ChR2 group (Fig. 7C; 87.29±1.67% for NTG mCherry vs 82.46±6.73% for APP ChR2), indicating that optogenetic treatment restored sleep-dependent memory consolidation in APP mice to that observed in NTG mice.

The same mice were subjected to a locomotor test to determine whether increases in freezing could be attributed to deficits in locomotor activity. The distance travelled in the open field was not significantly different for three groups (Fig. 7D; 2754±285.3cm for NTG mCherry vs 3329±285cm for APP mCherry vs 3125±346.1cm for APP ChR2). The average velocity of the APP mice did not show significant group differences (Fig. 7E; 4.59±0.48cm/s for NTG mCherry vs 5.61±0.47cm/s for APP mCherry vs 5.21±0.58cm/s for APP ChR2). Our data indicated that the locomotion of the APP mice was not impaired by optogenetic treatment. Thus, slow-wave rescue via optogenetic targeting of astrocytes improved sleep-dependent memory consolidation in APP mice.

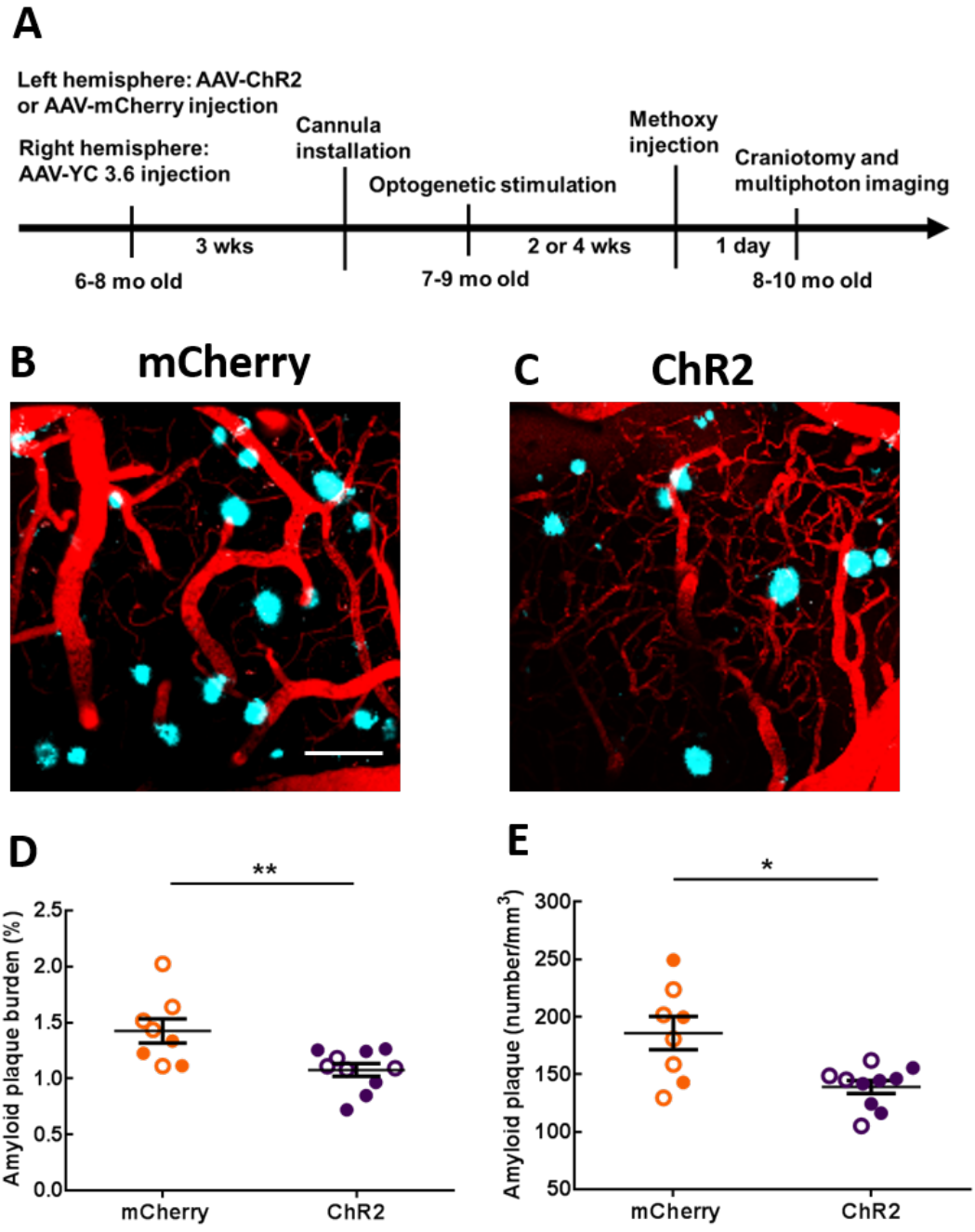

Figure 5: Slow-wave rescue decreases amyloid plaque deposition in APP mice. (A) Experimental design. (B, C) Representative multiphoton images of methoxy-X04 positive amyloid plaques after light activation of cortical astrocytes in mCherry (B) and ChR2 (C)

groups. (D) Amyloid plaque burden across conditions. (E) Amyloid plaque number across conditions. Values are presented as mean ± SEM. Males are represented by closed circles, and females by open circles. Scale bar, 100μm, *$p<0.05$, **$p<0.01$.

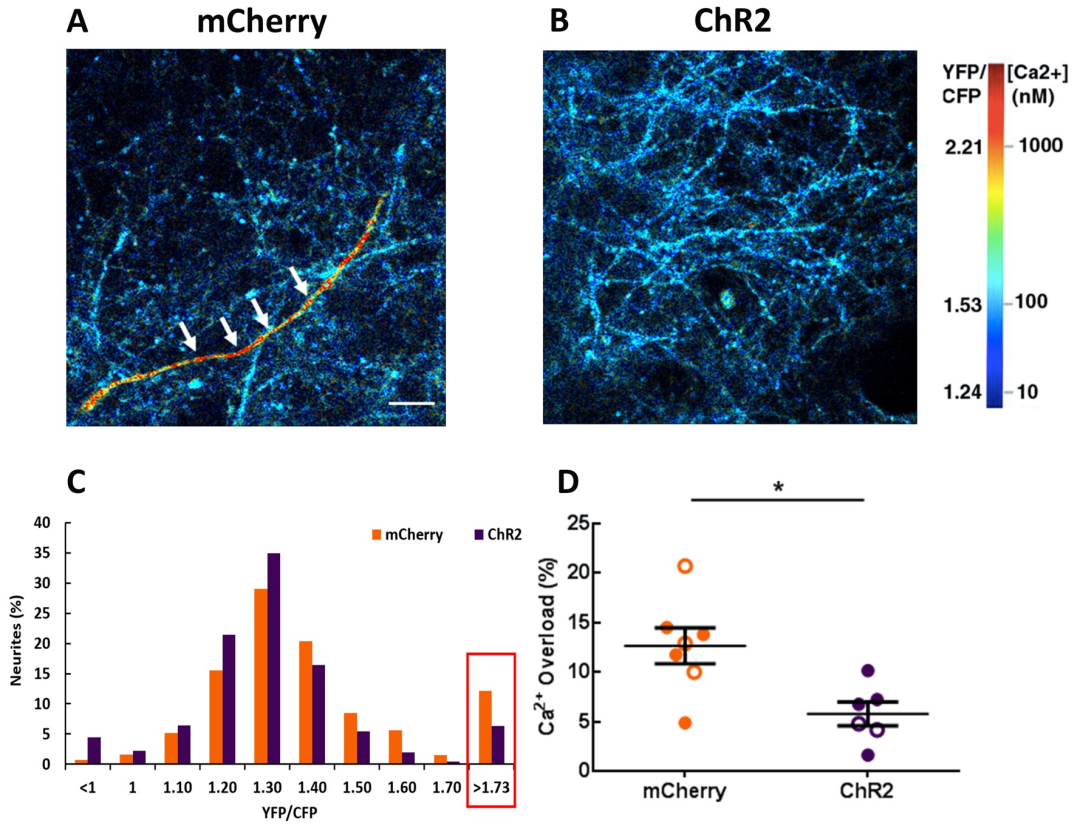

Figure 6: Optogenetic rescue normalizes neuronal calcium in APP mice. (A, B) The images pseudocolored according to the intraneuronal calcium concentration, acquired from APP mice expressing mCherry (A) or ChR2 (B). A neuronal process exhibiting calcium overload is seen in red (white arrows). (C) Histogram showing the distribution of YFP/CFP ratios in neurites expressing YC 3.6. Neuronal calcium overload was defined as a YFP/CFP ratio larger than 2 standard deviations above the average YFP/CFP ratio in the neurons of NTG mice. The ratio of YFP/CFP > 1.73 was considered as calcium overload. (D) The percentage of neurites exhibiting calcium overload after 2-4 weeks light activation of astrocytes. Values are mean ± SEM. Males are represented by closed circles and females by open circles. Scale bar, 100µm, *p<0.05.

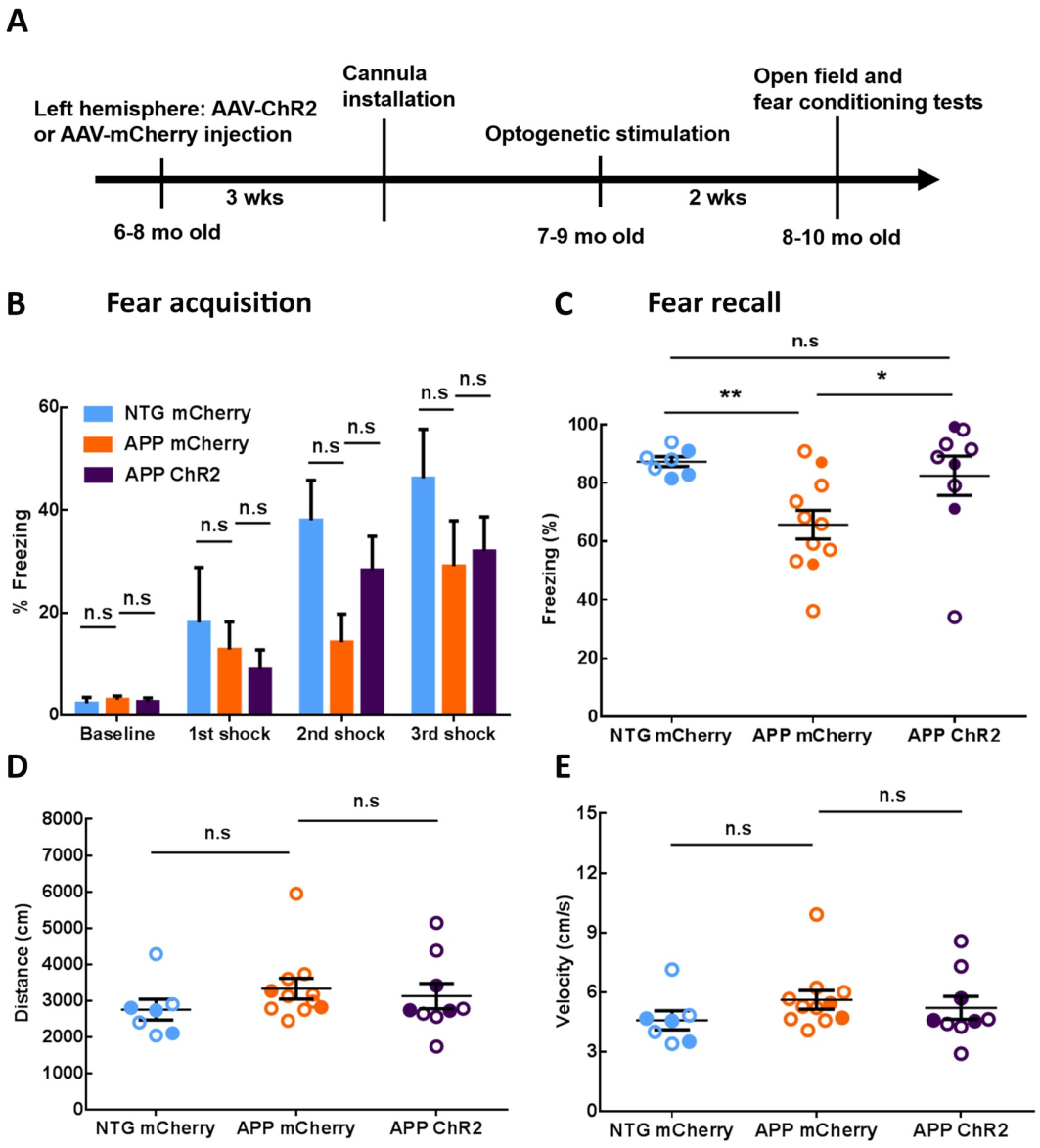

Figure 7: Optogenetic activation of astrocytes at the slow-wave frequency improves sleep-dependent memory performance in APP mice. (A) Experimental design. (B) Percentage of time spent freezing before and during fear conditioning. (C) Percentage of time spent freezing during fear recall. Sleep-dependent memory performance was assessed across groups. (D) The total distance traveled during open field test across

conditions. (E) The average velocity of movement during open field test across conditions. Values are mean ± SEM. Males are represented by closed circles, and females by open circles. n.s non-significant, *$p<0.05$, **$p<0.01$.

CHAPTER SIX: DISCUSSION

Patients with AD exhibit memory impairments and sleep disruptions. Slow oscillations, important for memory consolidation during sleep, are impaired in patients with AD and this feature is recapitulated in mouse models of beta-amyloidosis. Here we determined whether astrocytes contribute to slow-wave disruption in APP mice.

It is increasingly recognized that astrocytes, in addition to modulating local synaptic plasticity, control the activity of neural networks. Astrocytes actively participate in circuit function by interacting with pre- and post-synaptic neurons via tripartite synapses (Araque et al., 1999; Newman, 2003; Perea et al., 2009) and by communicating with neighboring astrocytes via gap junctions (Charles et al., 1991; Dani et al., 1992; Nedergaard, 1994). As each individual astrocyte interacts with thousands of neurons, they exhibit calcium transients indicative of the activity of the circuit in which that astrocyte is participating. We discovered aberrant calcium transients in astrocytes concomitant with aberrant slow oscillations in young APP mice, consistent with the reports of disrupted astrocytic calcium signaling in mouse models of beta-amyloidosis (Kuchibhotla et al., 2009; Lines et al., 2022). Compared to non-transgenic control mice, calcium transients in astrocytes of APP mice maintain the slow-wave frequency but show decreased power, starting at 3 months of age, before plaque deposition (Kastanenka et al., 2017). This suggests that disruption of astrocytic calcium transients is an early event in the disease progression.

Since astrocytic calcium transients were disrupted, we used optogenetics to stimulate cortical astrocytes at the slow-wave frequency to restore the SWA circuit in

APP mice. We showed that optogenetics allowed targeting of astrocytes with high fidelity and spatiotemporal precision within the intact cortico-thalamic circuit driving slow waves in vivo. Slow oscillations were restored by activation of ChR2-expressing astrocytes in APP mice. This suggests that even though slow oscillations are impaired, the glial-neuronal circuit remains intact.

The APP mice used here overexpress a human mutant APP transgene and a human mutant (presenilin 1) PS1 variant, generate Aβ and deposit amyloid plaques starting at 4.5-5 months of age (Garcia-Alloza et al., 2006). Accumulation of Aβ results in neuronal dysfunction and circuit impairments (Hardy & Higgins, 1992; Palop & Mucke, 2010; Selkoe & Hardy, 2016). Here we showed that optogenetic targeting of astrocytes to restore SWA decreased the rate of amyloid beta deposition in APP mice. Previous studies reported a link between Aβ production and SWA impairments in cognitively healthy adults (Ju et al., 2017; Lucey et al., 2019; Mander et al., 2015). Increased Aβ deposition within medial prefrontal cortex has been associated with decreased SWA (Mander et al., 2015). In addition, the levels of Aβ in cerebrospinal fluids increase after SWA suppression using auditory tones (Ju et al., 2017). Our finding that the alteration of astrocytic network function decreases amyloid plaque deposition serves to confirm and further expand on these previous results, and strongly suggests that astrocytes regulate slow oscillations and participate in the pathogenesis of AD.

Amyloid disrupts neuronal calcium homeostasis which results in calcium elevations. Abnormal neuronal calcium homeostasis has been reported in AD (Berridge, 2011; Bezprozvanny & Mattson, 2008; Henstridge et al., 2019) and transgenic mouse

models of beta-amyloidosis, such as APP and Tg2576 mice (Kastanenka et al., 2016, 2017; Kuchibhotla et al., 2008). The measure of basal neuronal calcium has been adopted as a functional readout of treatment efficacy in animal models of AD (Kastanenka et al., 2016; Lee et al., 2021; Pagnier et al., 2018; Wang et al., 2018). Indeed, we observed neurons with calcium elevations or calcium overload in APP mice (Kuchibhotla et al., 2008; Arbel-Ornath et al., 2017; Kastanenka et al., 2017). The toxicity of amyloid plaques or exchangeable oligomers surrounding plaques is likely responsible for the calcium overload in neurons, since the percentage of neurites exhibiting calcium overload is proportionally related to the proximity to plaques (Kuchibhotla et al., 2008). Furthermore, soluble oligomeric Aβ elicited pronounced calcium elevations in neurons *in vivo* (Arbel-Ornath et al., 2017; Wang et al., 2018). Our findings indicate that abnormal neuronal calcium elevations in APP mice are prevented by activating astrocytes with optogenetics. Slow-wave restoration in this manner decreased deposition of amyloid plaques and restored calcium homeostasis within neurons in APP mice. Therefore, calcium imaging of YC3.6-expressing neurons and astrocytes established a causal link between disruptions in sleep-dependent brain rhythms and Alzheimer's progression. In other words, dysfunction of SWA is not simply symptomatic of the disease but actively contributes to its progression. These studies highlight the potential of sleep-dependent brain rhythm recovery to slow disease progression.

Deficits in SWA result in memory impairments (Backhaus et al., 2007; Mander et al., 2013). Potentiation of SWA during sleep has been linked to improvements in declarative memory consolidation in human subjects (Ladenbauer et al., 2017; Marshall

et al., 2004, 2006; Westerberg et al., 2015). Restoration of SWA during NREM sleep in patients with AD might slow disease progression and rescue sleep-dependent memory consolidation. Transcranial direct current stimulation (tDCS) and transcranial magnetic stimulation (TMS) are two noninvasive brain stimulation methodologies that could potentially be used to do so. Recently, tDCS was applied to human MCI subjects during daytime nap to investigate the patterns of SWA and sleep-dependent memory consolidation. Both the slow oscillation power and memory performance were improved after stimulating the brain at the slow oscillation frequency at 0.75 Hz with tDCS (Ladenbauer et al., 2017). Furthermore, repeated applications of tDCS induced slow oscillations during SWS and led to enhanced declarative memory retention the next day in older (Westerberg et al., 2015) and in young healthy adults (Marshall et al., 2004, 2006). In a similar study, TMS was used to evoke slow waves during NREM sleep. TMS increased SWA power in healthy young subjects (Massimini et al., 2007). In addition to tDCS and TMS methodologies, slow oscillations can be enhanced with auditory stimulation (Leminen et al., 2017; Ngo et al., 2013; Ong et al., 2018; Papalambros et al., 2017). Applied auditory tones that were phase-locked to the UP states of slow oscillations during sleep benefited declarative memory consolidation in healthy young adults (Leminen et al., 2017; Ngo et al., 2013) and in older subjects (Papalambros et al., 2017). Furthermore, phase-locked acoustic stimulation also enhanced memory encoding during nap in healthy young subjects (Ong et al., 2018). Another sensory stimulation strategy, visual stimulation, can be used to induce SWA (Riedner et al., 2011). Using high-density EEG recordings in healthy young subjects during NREM sleep, SWA was successfully

evoked by visual stimuli (Riedner et al., 2011). Thus, tDCS, TMS, acoustic, and visual stimulations could potentially be used to enhance SWA and further improves sleep-dependent memory consolidation in healthy subjects and AD patients in early stages of the disease. Animal models of AD recapitulate the slow-wave disruptions and can be used for mechanistic studies. Use of leading-edge technologies, including optogenetics, intravital wide-field imaging and multiphoton microscopy, provided insight into the mechanisms of slow-wave disruptions in AD. In mice, this includes the impairment in contextual fear memory starting at 6 months of age (Kilgore et al., 2010). Here we monitored sleep-dependent memory consolidation in APP mice and saw improvements of fear recall but not fear acquisition after optogenetic treatment. This suggests that aberrant astrocytic function actively contributes to deficits in sleep-dependent memory consolidation. Furthermore, these data provide further evidence that disrupted slow oscillations contribute to memory decline in AD.

A better understanding of the relationship between SWA disruptions and memory decline may shed light on the mechanistic pathways underlying AD-associated memory impairment. Utilizing noninvasive brain stimulation technologies and medications that upregulate astrocytic activity of cortico-thalamic circuits may prove to become efficient therapeutic strategies. Development of novel therapeutic interventions targeting SWA during NREM sleep early in the disease progression might slow memory decline in the elderly and delay AD onset in MCI or healthy individuals at risk for developing AD. In summary, we demonstrate that astrocytes are critical for maintaining proper circuit function in APP mice. Restoration of SWA via astrocyte targeting reduces amyloid

plaque deposition, restores the calcium homeostasis in neurons, and improves sleep-dependent memory consolidation in APP mice. Our results provide evidence that dysfunctional slow oscillations underlie the memory impairments and pathophysiology of AD. Targeting astrocytes to alter SWA might serve as a novel therapeutic strategy against AD.

BIBLIOGRAPHY

Abbott, N. J., Pizzo, M. E., Preston, J. E., Janigro, D., & Thorne, R. G. (2018). The role of brain barriers in fluid movement in the CNS: Is there a "glymphatic" system? *Acta Neuropathologica*, *135*(3), 387–407. https://doi.org/10.1007/s00401-018-1812-4

Abdelfattah, A. S., Kawashima, T., Singh, A., Novak, O., Liu, H., Shuai, Y., Huang, Y.-C., Campagnola, L., Seeman, S. C., Yu, J., Zheng, J., Grimm, J. B., Patel, R., Friedrich, J., Mensh, B. D., Paninski, L., Macklin, J. J., Murphy, G. J., Podgorski, K., … Schreiter, E. R. (2019). Bright and photostable chemigenetic indicators for extended in vivo voltage imaging. *Science (New York, N.Y.)*, *365*(6454), 699–704. https://doi.org/10.1126/science.aav6416

Araque, A., Parpura, V., Sanzgiri, R. P., & Haydon, P. G. (1999). Tripartite synapses: Glia, the unacknowledged partner. *Trends in Neurosciences*, *22*(5), 208–215. https://doi.org/10.1016/s0166-2236(98)01349-6

Arbel-Ornath, M., Hudry, E., Boivin, J. R., Hashimoto, T., Takeda, S., Kuchibhotla, K. V., Hou, S., Lattarulo, C. R., Belcher, A. M., Shakerdge, N., Trujillo, P. B., Muzikansky, A., Betensky, R. A., Hyman, B. T., & Bacskai, B. J. (2017). Soluble oligomeric amyloid-β induces calcium dyshomeostasis that precedes synapse loss in the living mouse brain. *Molecular Neurodegeneration*, *12*(1), 27. https://doi.org/10.1186/s13024-017-0169-9

Aton, S. J., Seibt, J., Dumoulin, M., Jha, S. K., Steinmetz, N., Coleman, T., Naidoo, N., & Frank, M. G. (2009). Mechanisms of sleep-dependent consolidation of cortical plasticity. *Neuron*, *61*(3), 454–466. https://doi.org/10.1016/j.neuron.2009.01.007

Backhaus, J., Born, J., Hoeckesfeld, R., Fokuhl, S., Hohagen, F., & Junghanns, K. (2007). Midlife decline in declarative memory consolidation is correlated with a decline in slow wave sleep. *Learning & Memory (Cold Spring Harbor, N.Y.)*, *14*(5), 336–341. https://doi.org/10.1101/lm.470507

Backhaus, J., Junghanns, K., Born, J., Hohaus, K., Faasch, F., & Hohagen, F. (2006). Impaired declarative memory consolidation during sleep in patients with primary insomnia: Influence of sleep architecture and nocturnal cortisol release. *Biological Psychiatry*, *60*(12), 1324–1330. https://doi.org/10.1016/j.biopsych.2006.03.051

Bazhenov, M., Timofeev, I., Steriade, M., & Sejnowski, T. J. (2002). Model of thalamocortical slow-wave sleep oscillations and transitions to activated States. *The Journal of Neuroscience: The Official Journal of the Society for Neuroscience*, *22*(19), 8691–8704.

Beaulieu-Laroche, L., Toloza, E. H. S., van der Goes, M.-S., Lafourcade, M., Barnagian, D., Williams, Z. M., Eskandar, E. N., Frosch, M. P., Cash, S. S., & Harnett, M. T. (2018). Enhanced Dendritic Compartmentalization in Human Cortical Neurons. *Cell*, *175*(3), 643-651.e14. https://doi.org/10.1016/j.cell.2018.08.045

Berridge, M. J. (1998). Neuronal Calcium Signaling. *Neuron*, *21*(1), 13–26. https://doi.org/10.1016/S0896-6273(00)80510-3

Berridge, M. J. (2011). Calcium signalling and Alzheimer's disease. *Neurochemical Research*, *36*(7), 1149–1156. https://doi.org/10.1007/s11064-010-0371-4

Berridge, M. J. (2014). Calcium regulation of neural rhythms, memory and Alzheimer's disease. *The Journal of Physiology*, *592*(Pt 2), 281–293. https://doi.org/10.1113/jphysiol.2013.257527

Bezprozvanny, I., & Mattson, M. P. (2008). Neuronal calcium mishandling and the pathogenesis of Alzheimer's disease. *Trends in Neurosciences*, *31*(9), 454–463. https://doi.org/10.1016/j.tins.2008.06.005

Bliwise, D. L., Hughes, M., McMahon, P. M., & Kutner, N. (1995). Observed sleep/wakefulness and severity of dementia in an Alzheimer's disease special care unit. *The Journals of Gerontology. Series A, Biological Sciences and Medical Sciences*, *50*(6), M303-306. https://doi.org/10.1093/gerona/50a.6.m303

Bloom, G. S. (2014). Amyloid-β and tau: The trigger and bullet in Alzheimer disease pathogenesis. *JAMA Neurology*, *71*(4), 505–508. https://doi.org/10.1001/jamaneurol.2013.5847

Born, J. (2010). Slow-wave sleep and the consolidation of long-term memory. *The World Journal of Biological Psychiatry: The Official Journal of the World Federation of Societies of Biological Psychiatry*, *11 Suppl 1*, 16–21. https://doi.org/10.3109/15622971003637637

Born, J., & Wilhelm, I. (2012). System consolidation of memory during sleep. *Psychological Research*, *76*(2), 192–203. https://doi.org/10.1007/s00426-011-0335-6

Bouter, Y., Lopez Noguerola, J. S., Tucholla, P., Crespi, G. A. N., Parker, M. W., Wiltfang, J., Miles, L. A., & Bayer, T. A. (2015). Abeta targets of the biosimilar antibodies of Bapineuzumab, Crenezumab, Solanezumab in comparison to an antibody against N-truncated Abeta in sporadic Alzheimer disease cases and mouse models. *Acta Neuropathologica*, *130*(5), 713–729. https://doi.org/10.1007/s00401-015-1489-x

Boyden, E. S., Zhang, F., Bamberg, E., Nagel, G., & Deisseroth, K. (2005). Millisecond-timescale, genetically targeted optical control of neural activity. *Nature Neuroscience*, *8*(9), 1263–1268. https://doi.org/10.1038/nn1525

Brzecka, A., Leszek, J., Ashraf, G. M., Ejma, M., Ávila-Rodriguez, M. F., Yarla, N. S., Tarasov, V. V., Chubarev, V. N., Samsonova, A. N., Barreto, G. E., & Aliev, G. (2018). Sleep Disorders Associated With Alzheimer's Disease: A Perspective. *Frontiers in Neuroscience*, *12*, 330. https://doi.org/10.3389/fnins.2018.00330

Busche, M. A., Eichhoff, G., Adelsberger, H., Abramowski, D., Wiederhold, K.-H., Haass, C., Staufenbiel, M., Konnerth, A., & Garaschuk, O. (2008). Clusters of hyperactive neurons near amyloid plaques in a mouse model of Alzheimer's disease. *Science (New York, N.Y.)*, *321*(5896), 1686–1689. https://doi.org/10.1126/science.1162844

Busche, M. A., Kekuš, M., Adelsberger, H., Noda, T., Förstl, H., Nelken, I., & Konnerth, A. (2015). Rescue of long-range circuit dysfunction in Alzheimer's disease models. *Nature Neuroscience*, *18*(11), 1623–1630. https://doi.org/10.1038/nn.4137

Calderon-Garcidueñas, A. L., & Duyckaerts, C. (2018). Chapter 23—Alzheimer disease. In G. G. Kovacs & I. Alafuzoff (Eds.), *Handbook of Clinical Neurology* (Vol. 145, pp. 325–337). Elsevier. https://doi.org/10.1016/B978-0-12-802395-2.00023-7

Calvo-Rodriguez, M., Hou, S. S., Snyder, A. C., Kharitonova, E. K., Russ, A. N., Das, S., Fan, Z., Muzikansky, A., Garcia-Alloza, M., Serrano-Pozo, A., Hudry, E., & Bacskai, B. J. (2020). Increased mitochondrial calcium levels associated with neuronal death in a mouse model of Alzheimer's disease. *Nature Communications*, *11*(1), 2146. https://doi.org/10.1038/s41467-020-16074-2

Capani, F., Quarracino, C., Caccuri, R., & Sica, R. E. P. (2016). Astrocytes As the Main Players in Primary Degenerative Disorders of the Human Central Nervous System. *Frontiers in Aging Neuroscience*, *8*, 45. https://doi.org/10.3389/fnagi.2016.00045

Cash, S. S., Halgren, E., Dehghani, N., Rossetti, A. O., Thesen, T., Wang, C., Devinsky, O., Kuzniecky, R., Doyle, W., Madsen, J. R., Bromfield, E., Erőss, L., Halász, P., Karmos, G., Csercsa, R., Wittner, L., & Ulbert, I. (2009). The Human K-Complex Represents an Isolated Cortical Down-State. *Science (New York, N.Y.)*, *324*(5930), 1084–1087. https://doi.org/10.1126/science.1169626

Castano-Prat, P., Perez-Mendez, L., Perez-Zabalza, M., Sanfeliu, C., Giménez-Llort, L., & Sanchez-Vives, M. V. (2019). Altered slow (<1 Hz) and fast (beta and gamma)

neocortical oscillations in the 3xTg-AD mouse model of Alzheimer's disease under anesthesia. *Neurobiology of Aging*, *79*, 142–151. https://doi.org/10.1016/j.neurobiolaging.2019.02.009

Charles, A. C., Merrill, J. E., Dirksen, E. R., & Sanderson, M. J. (1991). Intercellular signaling in glial cells: Calcium waves and oscillations in response to mechanical stimulation and glutamate. *Neuron*, *6*(6), 983–992. https://doi.org/10.1016/0896-6273(91)90238-u

Chauvette, S., Seigneur, J., & Timofeev, I. (2012). Sleep oscillations in the thalamocortical system induce long-term neuronal plasticity. *Neuron*, *75*(6), 1105–1113. https://doi.org/10.1016/j.neuron.2012.08.034

Chauvette, S., Volgushev, M., & Timofeev, I. (2010). Origin of active states in local neocortical networks during slow sleep oscillation. *Cerebral Cortex (New York, N.Y.: 1991)*, *20*(11), 2660–2674. https://doi.org/10.1093/cercor/bhq009

Chen, J.-Y., Chauvette, S., Skorheim, S., Timofeev, I., & Bazhenov, M. (2012). Interneuron-mediated inhibition synchronizes neuronal activity during slow oscillation. *The Journal of Physiology*, *590*(16), 3987–4010. https://doi.org/10.1113/jphysiol.2012.227462

Chen, T.-W., Wardill, T. J., Sun, Y., Pulver, S. R., Renninger, S. L., Baohan, A., Schreiter, E. R., Kerr, R. A., Orger, M. B., Jayaraman, V., Looger, L. L., Svoboda, K., & Kim, D. S. (2013). Ultrasensitive fluorescent proteins for imaging neuronal activity. *Nature*, *499*(7458), 295–300. https://doi.org/10.1038/nature12354

Clarke, L. E., & Barres, B. A. (2013). Emerging roles of astrocytes in neural circuit development. *Nature Reviews. Neuroscience*, *14*(5), 311–321. https://doi.org/10.1038/nrn3484

Contreras, D., & Steriade, M. (1995). Cellular basis of EEG slow rhythms: A study of dynamic corticothalamic relationships. *The Journal of Neuroscience: The Official Journal of the Society for Neuroscience*, *15*(1 Pt 2), 604–622.

Csercsa, R., Dombovári, B., Fabó, D., Wittner, L., Eross, L., Entz, L., Sólyom, A., Rásonyi, G., Szucs, A., Kelemen, A., Jakus, R., Juhos, V., Grand, L., Magony, A., Halász, P., Freund, T. F., Maglóczky, Z., Cash, S. S., Papp, L., … Ulbert, I. (2010). Laminar analysis of slow wave activity in humans. *Brain: A Journal of Neurology*, *133*(9), 2814–2829. https://doi.org/10.1093/brain/awq169

Dana, H., Sun, Y., Mohar, B., Hulse, B. K., Kerlin, A. M., Hasseman, J. P., Tsegaye, G., Tsang, A., Wong, A., Patel, R., Macklin, J. J., Chen, Y., Konnerth, A., Jayaraman,

V., Looger, L. L., Schreiter, E. R., Svoboda, K., & Kim, D. S. (2019). High-performance calcium sensors for imaging activity in neuronal populations and microcompartments. *Nature Methods*, *16*(7), 649–657. https://doi.org/10.1038/s41592-019-0435-6

Dani, J. W., Chernjavsky, A., & Smith, S. J. (1992). Neuronal activity triggers calcium waves in hippocampal astrocyte networks. *Neuron*, *8*(3), 429–440. https://doi.org/10.1016/0896-6273(92)90271-e

David, F., Schmiedt, J. T., Taylor, H. L., Orban, G., Di Giovanni, G., Uebele, V. N., Renger, J. J., Lambert, R. C., Leresche, N., & Crunelli, V. (2013). Essential thalamic contribution to slow waves of natural sleep. *The Journal of Neuroscience: The Official Journal of the Society for Neuroscience*, *33*(50), 19599–19610. https://doi.org/10.1523/JNEUROSCI.3169-13.2013

DeKosky, S. T., & Scheff, S. W. (1990). Synapse loss in frontal cortex biopsies in Alzheimer's disease: Correlation with cognitive severity. *Annals of Neurology*, *27*(5), 457–464. https://doi.org/10.1002/ana.410270502

Diekelmann, S., & Born, J. (2010). The memory function of sleep. *Nature Reviews. Neuroscience*, *11*(2), 114–126. https://doi.org/10.1038/nrn2762

Etter, G., van der Veldt, S., Manseau, F., Zarrinkoub, I., Trillaud-Doppia, E., & Williams, S. (2019). Optogenetic gamma stimulation rescues memory impairments in an Alzheimer's disease mouse model. *Nature Communications*, *10*(1), 5322. https://doi.org/10.1038/s41467-019-13260-9

Fenno, L., Yizhar, O., & Deisseroth, K. (2011). The development and application of optogenetics. *Annual Review of Neuroscience*, *34*, 389–412. https://doi.org/10.1146/annurev-neuro-061010-113817

Fiáth, R., Kerekes, B. P., Wittner, L., Tóth, K., Beregszászi, P., Horváth, D., & Ulbert, I. (2016). Laminar analysis of the slow wave activity in the somatosensory cortex of anesthetized rats. *The European Journal of Neuroscience*, *44*(3), 1935–1951. https://doi.org/10.1111/ejn.13274

Förstl, H., & Kurz, A. (1999). Clinical features of Alzheimer's disease. *European Archives of Psychiatry and Clinical Neuroscience*, *249*(6), 288–290. https://doi.org/10.1007/s004060050101

Funk, C. M., Peelman, K., Bellesi, M., Marshall, W., Cirelli, C., & Tononi, G. (2017). Role of Somatostatin-Positive Cortical Interneurons in the Generation of Sleep Slow Waves. *The Journal of Neuroscience*, *37*(38), 9132–9148. https://doi.org/10.1523/JNEUROSCI.1303-17.2017

Garcia-Alloza, M., Robbins, E. M., Zhang-Nunes, S. X., Purcell, S. M., Betensky, R. A., Raju, S., Prada, C., Greenberg, S. M., Bacskai, B. J., & Frosch, M. P. (2006). Characterization of amyloid deposition in the APPswe/PS1dE9 mouse model of Alzheimer disease. *Neurobiology of Disease*, *24*(3), 516–524. https://doi.org/10.1016/j.nbd.2006.08.017

Gerashchenko, D., Schmidt, M. A., Zielinski, M. R., Moore, M. E., & Wisor, J. P. (2018). Sleep State Dependence of Optogenetically evoked Responses in Neuronal Nitric Oxide Synthase-positive Cells of the Cerebral Cortex. *Neuroscience*, *379*, 189–201. https://doi.org/10.1016/j.neuroscience.2018.02.006

Gerashchenko, D., Wisor, J. P., Burns, D., Reh, R. K., Shiromani, P. J., Sakurai, T., de la Iglesia, H. O., & Kilduff, T. S. (2008). Identification of a population of sleep-active cerebral cortex neurons. *Proceedings of the National Academy of Sciences of the United States of America*, *105*(29), 10227–10232. https://doi.org/10.1073/pnas.0803125105

Giovannetti, E. A., Poll, S., Justus, D., Kaneko, H., Fuhrmann, F., Steffen, J., Remy, S., & Fuhrmann, M. (2018). *Restoring memory by optogenetic synchronization of hippocampal oscillations in an Alzheimer's disease mouse model* (p. 363820). bioRxiv. https://doi.org/10.1101/363820

Green, K. N., & LaFerla, F. M. (2008). Linking calcium to Abeta and Alzheimer's disease. *Neuron*, *59*(2), 190–194. https://doi.org/10.1016/j.neuron.2008.07.013

Haider, B., Duque, A., Hasenstaub, A. R., & McCormick, D. A. (2006). Neocortical network activity in vivo is generated through a dynamic balance of excitation and inhibition. *The Journal of Neuroscience: The Official Journal of the Society for Neuroscience*, *26*(17), 4535–4545. https://doi.org/10.1523/JNEUROSCI.5297-05.2006

Haider, B., Häusser, M., & Carandini, M. (2013). Inhibition dominates sensory responses in the awake cortex. *Nature*, *493*(7430), 97–100. https://doi.org/10.1038/nature11665

Haider, B., & McCormick, D. A. (2009). Rapid neocortical dynamics: Cellular and network mechanisms. *Neuron*, *62*(2), 171–189. https://doi.org/10.1016/j.neuron.2009.04.008

Hardy, J. A., & Higgins, G. A. (1992). Alzheimer's disease: The amyloid cascade hypothesis. *Science (New York, N.Y.)*, *256*(5054), 184–185. https://doi.org/10.1126/science.1566067

Haydon, P. G., & Carmignoto, G. (2006). Astrocyte Control of Synaptic Transmission and Neurovascular Coupling. *Physiological Reviews*, *86*(3), 1009–1031. https://doi.org/10.1152/physrev.00049.2005

Henstridge, C. M., Hyman, B. T., & Spires-Jones, T. L. (2019). Beyond the neuron–cellular interactions early in Alzheimer disease pathogenesis. *Nature Reviews Neuroscience*, *20*(2), 94–108. https://doi.org/10.1038/s41583-018-0113-1

Hijazi, S., Heistek, T. S., Scheltens, P., Neumann, U., Shimshek, D. R., Mansvelder, H. D., Smit, A. B., & van Kesteren, R. E. (2020). Early restoration of parvalbumin interneuron activity prevents memory loss and network hyperexcitability in a mouse model of Alzheimer's disease. *Molecular Psychiatry*, *25*(12), 3380–3398. https://doi.org/10.1038/s41380-019-0483-4

Hinard, V., Mikhail, C., Pradervand, S., Curie, T., Houtkooper, R. H., Auwerx, J., Franken, P., & Tafti, M. (2012). Key electrophysiological, molecular, and metabolic signatures of sleep and wakefulness revealed in primary cortical cultures. *The Journal of Neuroscience: The Official Journal of the Society for Neuroscience*, *32*(36), 12506–12517. https://doi.org/10.1523/JNEUROSCI.2306-12.2012

Holth, J. K., Mahan, T. E., Robinson, G. O., Rocha, A., & Holtzman, D. M. (2017). Altered sleep and EEG power in the P301S Tau transgenic mouse model. *Annals of Clinical and Translational Neurology*, *4*(3), 180–190. https://doi.org/10.1002/acn3.390

Iaccarino, H. F., Singer, A. C., Martorell, A. J., Rudenko, A., Gao, F., Gillingham, T. Z., Mathys, H., Seo, J., Kritskiy, O., Abdurrob, F., Adaikkan, C., Canter, R. G., Rueda, R., Brown, E. N., Boyden, E. S., & Tsai, L.-H. (2016). Gamma frequency entrainment attenuates amyloid load and modifies microglia. *Nature*, *540*(7632), 230–235. https://doi.org/10.1038/nature20587

Iliff, J. J., Wang, M., Liao, Y., Plogg, B. A., Peng, W., Gundersen, G. A., Benveniste, H., Vates, G. E., Deane, R., Goldman, S. A., Nagelhus, E. A., & Nedergaard, M. (2012). A paravascular pathway facilitates CSF flow through the brain parenchyma and the clearance of interstitial solutes, including amyloid β. *Science Translational Medicine*, *4*(147), 147ra111. https://doi.org/10.1126/scitranslmed.3003748

Jankowsky, J. L., Slunt, H. H., Ratovitski, T., Jenkins, N. A., Copeland, N. G., & Borchelt, D. R. (2001). Co-expression of multiple transgenes in mouse CNS: A comparison of strategies. *Biomolecular Engineering*, *17*(6), 157–165. https://doi.org/10.1016/s1389-0344(01)00067-3

Jasinska, M., Grzegorczyk, A., Woznicka, O., Jasek, E., Kossut, M., Barbacka-Surowiak, G., Litwin, J. A., & Pyza, E. (2015). Circadian rhythmicity of synapses in mouse somatosensory cortex. *European Journal of Neuroscience*, *42*(8), 2585–2594. https://doi.org/10.1111/ejn.13045

Ju, Y.-E. S., McLeland, J. S., Toedebusch, C. D., Xiong, C., Fagan, A. M., Duntley, S. P., Morris, J. C., & Holtzman, D. M. (2013). Sleep quality and preclinical Alzheimer disease. *JAMA Neurology*, *70*(5), 587–593. https://doi.org/10.1001/jamaneurol.2013.2334

Ju, Y.-E. S., Ooms, S. J., Sutphen, C., Macauley, S. L., Zangrilli, M. A., Jerome, G., Fagan, A. M., Mignot, E., Zempel, J. M., Claassen, J. A. H. R., & Holtzman, D. M. (2017). Slow wave sleep disruption increases cerebrospinal fluid amyloid-β levels. *Brain: A Journal of Neurology*, *140*(8), 2104–2111. https://doi.org/10.1093/brain/awx148

Kang, J.-E., Lim, M. M., Bateman, R. J., Lee, J. J., Smyth, L. P., Cirrito, J. R., Fujiki, N., Nishino, S., & Holtzman, D. M. (2009). Amyloid-beta dynamics are regulated by orexin and the sleep-wake cycle. *Science (New York, N.Y.)*, *326*(5955), 1005–1007. https://doi.org/10.1126/science.1180962

Kastanenka, K. V., Bussiere, T., Shakerdge, N., Qian, F., Weinreb, P. H., Rhodes, K., & Bacskai, B. J. (2016). Immunotherapy with Aducanumab Restores Calcium Homeostasis in Tg2576 Mice. *The Journal of Neuroscience: The Official Journal of the Society for Neuroscience*, *36*(50), 12549–12558. https://doi.org/10.1523/JNEUROSCI.2080-16.2016

Kastanenka, K. V., Calvo-Rodriguez, M., Hou, S. S., Zhou, H., Takeda, S., Arbel-Ornath, M., Lariviere, A., Lee, Y. F., Kim, A., Hawkes, J. M., Logan, R., Feng, D., Chen, X., Gomperts, S. N., & Bacskai, B. J. (2019). Frequency-dependent exacerbation of Alzheimer's disease neuropathophysiology. *Scientific Reports*, *9*(1), 8964. https://doi.org/10.1038/s41598-019-44964-z

Kastanenka, K. V., Hou, S. S., Shakerdge, N., Logan, R., Feng, D., Wegmann, S., Chopra, V., Hawkes, J. M., Chen, X., & Bacskai, B. J. (2017). Optogenetic Restoration of Disrupted Slow Oscillations Halts Amyloid Deposition and Restores Calcium Homeostasis in an Animal Model of Alzheimer's Disease. *PloS One*, *12*(1), e0170275. https://doi.org/10.1371/journal.pone.0170275

Kastanenka, K. V., Moreno-Bote, R., De Pittà, M., Perea, G., Eraso-Pichot, A., Masgrau, R., Poskanzer, K. E., & Galea, E. (2020). A roadmap to integrate astrocytes into Systems Neuroscience. *Glia*, *68*(1), 5–26. https://doi.org/10.1002/glia.23632

Kent, B. A., Strittmatter, S. M., & Nygaard, H. B. (2018). Sleep and EEG Power Spectral Analysis in Three Transgenic Mouse Models of Alzheimer's Disease: APP/PS1, 3xTgAD, and Tg2576. *Journal of Alzheimer's Disease : JAD*, *64*(4), 1325–1336. https://doi.org/10.3233/JAD-180260

Khachaturian, Z. S. (1994). Calcium hypothesis of Alzheimer's disease and brain aging. *Annals of the New York Academy of Sciences*, *747*, 1–11. https://doi.org/10.1111/j.1749-6632.1994.tb44398.x

Kilgore, M., Miller, C. A., Fass, D. M., Hennig, K. M., Haggarty, S. J., Sweatt, J. D., & Rumbaugh, G. (2010). Inhibitors of class 1 histone deacetylases reverse contextual memory deficits in a mouse model of Alzheimer's disease. *Neuropsychopharmacology: Official Publication of the American College of Neuropsychopharmacology*, *35*(4), 870–880. https://doi.org/10.1038/npp.2009.197

Kuchibhotla, K. V., Goldman, S. T., Lattarulo, C. R., Wu, H.-Y., Hyman, B. T., & Bacskai, B. J. (2008). Abeta plaques lead to aberrant regulation of calcium homeostasis in vivo resulting in structural and functional disruption of neuronal networks. *Neuron*, *59*(2), 214–225. https://doi.org/10.1016/j.neuron.2008.06.008

Kuchibhotla, K. V., Lattarulo, C. R., Hyman, B. T., & Bacskai, B. J. (2009). Synchronous hyperactivity and intercellular calcium waves in astrocytes in Alzheimer mice. *Science (New York, N.Y.)*, *323*(5918), 1211–1215. https://doi.org/10.1126/science.1169096

Ladenbauer, J., Ladenbauer, J., Külzow, N., de Boor, R., Avramova, E., Grittner, U., & Flöel, A. (2017). Promoting Sleep Oscillations and Their Functional Coupling by Transcranial Stimulation Enhances Memory Consolidation in Mild Cognitive Impairment. *The Journal of Neuroscience: The Official Journal of the Society for Neuroscience*, *37*(30), 7111–7124. https://doi.org/10.1523/JNEUROSCI.0260-17.2017

Lee, Y. F., Lariviere, L., Russ, A. N., Choi, S.-Z., Bacskai, B. J., & Kastanenka, K. V. (2021). Novel Botanical Therapeutic NB-02 Effectively Treats Alzheimer's Neuropathophysiology in an APP/PS1 Mouse Model. *ENeuro*, *8*(3), ENEURO.0389-20.2021. https://doi.org/10.1523/ENEURO.0389-20.2021

Lemieux, M., Chauvette, S., & Timofeev, I. (2015). Neocortical inhibitory activities and long-range afferents contribute to the synchronous onset of silent states of the neocortical slow oscillation. *Journal of Neurophysiology*, *113*(3), 768–779. https://doi.org/10.1152/jn.00858.2013

Lemieux, M., Chen, J.-Y., Lonjers, P., Bazhenov, M., & Timofeev, I. (2014). The impact of cortical deafferentation on the neocortical slow oscillation. *The Journal of Neuroscience: The Official Journal of the Society for Neuroscience*, *34*(16), 5689–5703. https://doi.org/10.1523/JNEUROSCI.1156-13.2014

Leminen, M. M., Virkkala, J., Saure, E., Paajanen, T., Zee, P. C., Santostasi, G., Hublin, C., Müller, K., Porkka-Heiskanen, T., Huotilainen, M., & Paunio, T. (2017). Enhanced Memory Consolidation Via Automatic Sound Stimulation During Non-REM Sleep. *Sleep*, *40*(3). https://doi.org/10.1093/sleep/zsx003

Li, X., Gutierrez, D. V., Hanson, M. G., Han, J., Mark, M. D., Chiel, H., Hegemann, P., Landmesser, L. T., & Herlitze, S. (2005). Fast noninvasive activation and inhibition of neural and network activity by vertebrate rhodopsin and green algae channelrhodopsin. *Proceedings of the National Academy of Sciences of the United States of America*, *102*(49), 17816–17821. https://doi.org/10.1073/pnas.0509030102

Lines, J., Baraibar, A. M., Fang, C., Martin, E. D., Aguilar, J., Lee, M. K., Araque, A., & Kofuji, P. (2022). Astrocyte-neuronal network interplay is disrupted in Alzheimer's disease mice. *Glia*, *70*(2), 368–378. https://doi.org/10.1002/glia.24112

Lu, W., & Göder, R. (2012). Does abnormal non-rapid eye movement sleep impair declarative memory consolidation?: Disturbed thalamic functions in sleep and memory processing. *Sleep Medicine Reviews*, *16*(4), 389–394. https://doi.org/10.1016/j.smrv.2011.08.001

Lucey, B. P., Mawuenyega, K. G., Patterson, B. W., Elbert, D. L., Ovod, V., Kasten, T., Morris, J. C., & Bateman, R. J. (2017). Associations Between β-Amyloid Kinetics and the β-Amyloid Diurnal Pattern in the Central Nervous System. *JAMA Neurology*, *74*(2), 207–215. https://doi.org/10.1001/jamaneurol.2016.4202

Lucey, B. P., McCullough, A., Landsness, E. C., Toedebusch, C. D., McLeland, J. S., Zaza, A. M., Fagan, A. M., McCue, L., Xiong, C., Morris, J. C., Benzinger, T. L. S., & Holtzman, D. M. (2019). Reduced non-rapid eye movement sleep is associated with tau pathology in early Alzheimer's disease. *Science Translational Medicine*, *11*(474), eaau6550. https://doi.org/10.1126/scitranslmed.aau6550

Mander, B. A., Marks, S. M., Vogel, J. W., Rao, V., Lu, B., Saletin, J. M., Ancoli-Israel, S., Jagust, W. J., & Walker, M. P. (2015). β-amyloid disrupts human NREM slow waves and related hippocampus-dependent memory consolidation. *Nature Neuroscience*, *18*(7), 1051–1057. https://doi.org/10.1038/nn.4035

Mander, B. A., Rao, V., Lu, B., Saletin, J. M., Lindquist, J. R., Ancoli-Israel, S., Jagust, W., & Walker, M. P. (2013). Prefrontal atrophy, disrupted NREM slow waves and impaired hippocampal-dependent memory in aging. *Nature Neuroscience*, *16*(3), 357–364. https://doi.org/10.1038/nn.3324

Marshall, L., Helgadóttir, H., Mölle, M., & Born, J. (2006). Boosting slow oscillations during sleep potentiates memory. *Nature*, *444*(7119), 610–613. https://doi.org/10.1038/nature05278

Marshall, L., Mölle, M., Hallschmid, M., & Born, J. (2004). Transcranial direct current stimulation during sleep improves declarative memory. *The Journal of Neuroscience: The Official Journal of the Society for Neuroscience*, *24*(44), 9985–9992. https://doi.org/10.1523/JNEUROSCI.2725-04.2004

Massimini, M., Ferrarelli, F., Esser, S. K., Riedner, B. A., Huber, R., Murphy, M., Peterson, M. J., & Tononi, G. (2007). Triggering sleep slow waves by transcranial magnetic stimulation. *Proceedings of the National Academy of Sciences of the United States of America*, *104*(20), 8496–8501. https://doi.org/10.1073/pnas.0702495104

Massimini, M., Huber, R., Ferrarelli, F., Hill, S., & Tononi, G. (2004). The Sleep Slow Oscillation as a Traveling Wave. *The Journal of Neuroscience*, *24*(31), 6862–6870. https://doi.org/10.1523/JNEUROSCI.1318-04.2004

McCurry, S. M., Logsdon, R. G., Teri, L., Gibbons, L. E., Kukull, W. A., Bowen, J. D., McCormick, W. C., & Larson, E. B. (1999). Characteristics of sleep disturbance in community-dwelling Alzheimer's disease patients. *Journal of Geriatric Psychiatry and Neurology*, *12*(2), 53–59. https://doi.org/10.1177/089198879901200203

Milojkovic, B. A., Zhou, W.-L., & Antic, S. D. (2007). Voltage and calcium transients in basal dendrites of the rat prefrontal cortex. *The Journal of Physiology*, *585*(Pt 2), 447–468. https://doi.org/10.1113/jphysiol.2007.142315

Miyamoto, D., Hirai, D., Fung, C. C. A., Inutsuka, A., Odagawa, M., Suzuki, T., Boehringer, R., Adaikkan, C., Matsubara, C., Matsuki, N., Fukai, T., McHugh, T. J., Yamanaka, A., & Murayama, M. (2016). Top-down cortical input during NREM sleep consolidates perceptual memory. *Science (New York, N.Y.)*, *352*(6291), 1315–1318. https://doi.org/10.1126/science.aaf0902

Miyawaki, A., Llopis, J., Heim, R., McCaffery, J. M., Adams, J. A., Ikura, M., & Tsien, R. Y. (1997). Fluorescent indicators for Ca2+ based on green fluorescent proteins and calmodulin. *Nature*, *388*(6645), 882–887. https://doi.org/10.1038/42264

Moe, K. E., Vitiello, M. V., Larsen, L. H., & Prinz, P. N. (1995). Symposium: Cognitive processes and sleep disturbances: Sleep/wake patterns in Alzheimer's disease: relationships with cognition and function. *Journal of Sleep Research*, *4*(1), 15–20. https://doi.org/10.1111/j.1365-2869.1995.tb00145.x

Mohajerani, M. H., McVea, D. A., Fingas, M., & Murphy, T. H. (2010). Mirrored bilateral slow-wave cortical activity within local circuits revealed by fast bihemispheric voltage-sensitive dye imaging in anesthetized and awake mice. *The Journal of Neuroscience: The Official Journal of the Society for Neuroscience*, *30*(10), 3745–3751. https://doi.org/10.1523/JNEUROSCI.6437-09.2010

Mohan, H., Verhoog, M. B., Doreswamy, K. K., Eyal, G., Aardse, R., Lodder, B. N., Goriounova, N. A., Asamoah, B., Brakspear, A. B., Groot, C., van der Sluis, S., Testa-Silva, G., Obermayer, J. M. G., Boudewijns, Z. S. R. M., Narayanan, R. T., Baayen, J. C., Segev, I., Mansvelder, H. D., & de Kock, C. P. J. (2015). Dendritic and Axonal Architecture of Individual Pyramidal Neurons across Layers of Adult Human Neocortex. *Cerebral Cortex (New York, N.Y. : 1991)*, *25*(12), 4839–4853. https://doi.org/10.1093/cercor/bhv188

Moran, M., Lynch, C. A., Walsh, C., Coen, R., Coakley, D., & Lawlor, B. A. (2005). Sleep disturbance in mild to moderate Alzheimer's disease. *Sleep Medicine*, *6*(4), 347–352. https://doi.org/10.1016/j.sleep.2004.12.005

Nagai, T., Yamada, S., Tominaga, T., Ichikawa, M., & Miyawaki, A. (2004). Expanded dynamic range of fluorescent indicators for Ca(2+) by circularly permuted yellow fluorescent proteins. *Proceedings of the National Academy of Sciences of the United States of America*, *101*(29), 10554–10559. https://doi.org/10.1073/pnas.0400417101

Nakai, J., Ohkura, M., & Imoto, K. (2001). A high signal-to-noise Ca(2+) probe composed of a single green fluorescent protein. *Nature Biotechnology*, *19*(2), 137–141. https://doi.org/10.1038/84397

Narikiyo, K., Mizuguchi, R., Ajima, A., Shiozaki, M., Hamanaka, H., Johansen, J. P., Mori, K., & Yoshihara, Y. (2020). The claustrum coordinates cortical slow-wave activity. *Nature Neuroscience*, *23*(6), 741–753. https://doi.org/10.1038/s41593-020-0625-7

Nedergaard, M. (1994). Direct signaling from astrocytes to neurons in cultures of mammalian brain cells. *Science (New York, N.Y.)*, *263*(5154), 1768–1771. https://doi.org/10.1126/science.8134839

Newman, E. A. (2003). New roles for astrocytes: Regulation of synaptic transmission. *Trends in Neurosciences*, *26*(10), 536–542. https://doi.org/10.1016/S0166-2236(03)00237-6

Ngo, H.-V. V., Martinetz, T., Born, J., & Mölle, M. (2013). Auditory closed-loop stimulation of the sleep slow oscillation enhances memory. *Neuron*, *78*(3), 545–553. https://doi.org/10.1016/j.neuron.2013.03.006

Niethard, N., Ngo, H.-V. V., Ehrlich, I., & Born, J. (2018). Cortical circuit activity underlying sleep slow oscillations and spindles. *Proceedings of the National Academy of Sciences of the United States of America*, *115*(39), E9220–E9229. https://doi.org/10.1073/pnas.1805517115

Ong, J. L., Patanaik, A., Chee, N. I. Y. N., Lee, X. K., Poh, J.-H., & Chee, M. W. L. (2018). Auditory stimulation of sleep slow oscillations modulates subsequent memory encoding through altered hippocampal function. *Sleep*, *41*(5), zsy031. https://doi.org/10.1093/sleep/zsy031

Pagnier, G. J., Kastanenka, K. V., Sohn, M., Choi, S., Choi, S.-H., Soh, H., & Bacskai, B. J. (2018). Novel botanical drug DA-9803 prevents deficits in Alzheimer's mouse models. *Alzheimer's Research & Therapy*, *10*(1), 11. https://doi.org/10.1186/s13195-018-0338-2

Palop, J. J., & Mucke, L. (2010). Amyloid-beta-induced neuronal dysfunction in Alzheimer's disease: From synapses toward neural networks. *Nature Neuroscience*, *13*(7), 812–818. https://doi.org/10.1038/nn.2583

Papalambros, N. A., Santostasi, G., Malkani, R. G., Braun, R., Weintraub, S., Paller, K. A., & Zee, P. C. (2017). Acoustic Enhancement of Sleep Slow Oscillations and Concomitant Memory Improvement in Older Adults. *Frontiers in Human Neuroscience*, *11*, 109. https://doi.org/10.3389/fnhum.2017.00109

Pasti, L., Volterra, A., Pozzan, T., & Carmignoto, G. (1997). Intracellular calcium oscillations in astrocytes: A highly plastic, bidirectional form of communication between neurons and astrocytes in situ. *The Journal of Neuroscience: The Official Journal of the Society for Neuroscience*, *17*(20), 7817–7830.

Perea, G., Navarrete, M., & Araque, A. (2009). Tripartite synapses: Astrocytes process and control synaptic information. *Trends in Neurosciences*, *32*(8), 421–431. https://doi.org/10.1016/j.tins.2009.05.001

Persechini, A., Lynch, J. A., & Romoser, V. A. (1997). Novel fluorescent indicator proteins for monitoring free intracellular Ca2+. *Cell Calcium*, *22*(3), 209–216. https://doi.org/10.1016/s0143-4160(97)90014-2

Phatnani, H., & Maniatis, T. (2015). Astrocytes in neurodegenerative disease. *Cold Spring Harbor Perspectives in Biology*, *7*(6), a020628. https://doi.org/10.1101/cshperspect.a020628

Poskanzer, K. E., & Yuste, R. (2011). Astrocytic regulation of cortical UP states. *Proceedings of the National Academy of Sciences of the United States of America*, *108*(45), 18453–18458. https://doi.org/10.1073/pnas.1112378108

Poskanzer, K. E., & Yuste, R. (2016). Astrocytes regulate cortical state switching in vivo. *Proceedings of the National Academy of Sciences of the United States of America*, *113*(19), E2675-2684. https://doi.org/10.1073/pnas.1520759113

Prinz, P. N., Vitaliano, P. P., Vitiello, M. V., Bokan, J., Raskind, M., Peskind, E., & Gerber, C. (1982). Sleep, EEG and mental function changes in senile dementia of the Alzheimer's type. *Neurobiology of Aging*, *3*(4), 361–370. https://doi.org/10.1016/0197-4580(82)90024-0

Rasch, B., & Born, J. (2013). About Sleep's Role in Memory. *Physiological Reviews*, *93*(2), 681–766. https://doi.org/10.1152/physrev.00032.2012

Riedner, B. A., Hulse, B. K., Murphy, M. J., Ferrarelli, F., & Tononi, G. (2011). Temporal dynamics of cortical sources underlying spontaneous and peripherally evoked slow waves. *Progress in Brain Research*, *193*, 201–218. https://doi.org/10.1016/B978-0-444-53839-0.00013-2

Robinson, S. R. (2000). Neuronal expression of glutamine synthetase in Alzheimer's disease indicates a profound impairment of metabolic interactions with astrocytes. *Neurochemistry International*, *36*(4–5), 471–482. https://doi.org/10.1016/s0197-0186(99)00150-3

Roh, J. H., Huang, Y., Bero, A. W., Kasten, T., Stewart, F. R., Bateman, R. J., & Holtzman, D. M. (2012). Sleep-wake cycle and diurnal fluctuation of amyloid-β as biomarkers of brain amyloid pathology. *Science Translational Medicine*, *4*(150), 150ra122. https://doi.org/10.1126/scitranslmed.3004291

Romoser, V. A., Hinkle, P. M., & Persechini, A. (1997). Detection in living cells of Ca2+-dependent changes in the fluorescence emission of an indicator composed of two green fluorescent protein variants linked by a calmodulin-binding sequence. A new class of fluorescent indicators. *The Journal of Biological Chemistry*, *272*(20), 13270–13274. https://doi.org/10.1074/jbc.272.20.13270

Roy, D. S., Arons, A., Mitchell, T. I., Pignatelli, M., Ryan, T. J., & Tonegawa, S. (2016). Memory retrieval by activating engram cells in mouse models of early

Alzheimer's disease. *Nature*, *531*(7595), 508–512. https://doi.org/10.1038/nature17172

Rudolph, M., Pospischil, M., Timofeev, I., & Destexhe, A. (2007). Inhibition determines membrane potential dynamics and controls action potential generation in awake and sleeping cat cortex. *The Journal of Neuroscience: The Official Journal of the Society for Neuroscience*, *27*(20), 5280–5290. https://doi.org/10.1523/JNEUROSCI.4652-06.2007

Sanchez-Vives, M. V., Mattia, M., Compte, A., Perez-Zabalza, M., Winograd, M., Descalzo, V. F., & Reig, R. (2010). Inhibitory modulation of cortical up states. *Journal of Neurophysiology*, *104*(3), 1314–1324. https://doi.org/10.1152/jn.00178.2010

Sanchez-Vives, M. V., & McCormick, D. A. (2000). Cellular and network mechanisms of rhythmic recurrent activity in neocortex. *Nature Neuroscience*, *3*(10), 1027–1034. https://doi.org/10.1038/79848

Schallier, A., Smolders, I., Van Dam, D., Loyens, E., De Deyn, P. P., Michotte, A., Michotte, Y., & Massie, A. (2011). Region- and age-specific changes in glutamate transport in the AβPP23 mouse model for Alzheimer's disease. *Journal of Alzheimer's Disease: JAD*, *24*(2), 287–300. https://doi.org/10.3233/JAD-2011-101005

Seibt, J., Dumoulin, M. C., Aton, S. J., Coleman, T., Watson, A., Naidoo, N., & Frank, M. G. (2012). Protein synthesis during sleep consolidates cortical plasticity in vivo. *Current Biology: CB*, *22*(8), 676–682. https://doi.org/10.1016/j.cub.2012.02.016

Seibt, J., & Frank, M. G. (2019). Primed to Sleep: The Dynamics of Synaptic Plasticity Across Brain States. *Frontiers in Systems Neuroscience*, *13*, 2. https://doi.org/10.3389/fnsys.2019.00002

Seibt, J., Richard, C. J., Sigl-Glöckner, J., Takahashi, N., Kaplan, D. I., Doron, G., de Limoges, D., Bocklisch, C., & Larkum, M. E. (2017). Cortical dendritic activity correlates with spindle-rich oscillations during sleep in rodents. *Nature Communications*, *8*(1), 684. https://doi.org/10.1038/s41467-017-00735-w

Selkoe, D. J. (2019). Early network dysfunction in Alzheimer's disease. *Science (New York, N.Y.)*, *365*(6453), 540–541. https://doi.org/10.1126/science.aay5188

Selkoe, D. J., & Hardy, J. (2016). The amyloid hypothesis of Alzheimer's disease at 25 years. *EMBO Molecular Medicine*, *8*(6), 595–608. https://doi.org/10.15252/emmm.201606210

Sevigny, J., Chiao, P., Bussière, T., Weinreb, P. H., Williams, L., Maier, M., Dunstan, R., Salloway, S., Chen, T., Ling, Y., O'Gorman, J., Qian, F., Arastu, M., Li, M., Chollate, S., Brennan, M. S., Quintero-Monzon, O., Scannevin, R. H., Arnold, H. M., … Sandrock, A. (2016). The antibody aducanumab reduces Aβ plaques in Alzheimer's disease. *Nature*, *537*(7618), 50–56. https://doi.org/10.1038/nature19323

Sheroziya, M., & Timofeev, I. (2014). Global intracellular slow-wave dynamics of the thalamocortical system. *The Journal of Neuroscience: The Official Journal of the Society for Neuroscience*, *34*(26), 8875–8893. https://doi.org/10.1523/JNEUROSCI.4460-13.2014

Spira, A. P., Gamaldo, A. A., An, Y., Wu, M. N., Simonsick, E. M., Bilgel, M., Zhou, Y., Wong, D. F., Ferrucci, L., & Resnick, S. M. (2013). Self-reported sleep and β-amyloid deposition in community-dwelling older adults. *JAMA Neurology*, *70*(12), 1537–1543. https://doi.org/10.1001/jamaneurol.2013.4258

Spires-Jones, T. L., & Hyman, B. T. (2014). The intersection of amyloid beta and tau at synapses in Alzheimer's disease. *Neuron*, *82*(4), 756–771. https://doi.org/10.1016/j.neuron.2014.05.004

Steriade, M., Contreras, D., Curró Dossi, R., & Nuñez, A. (1993). The slow (< 1 Hz) oscillation in reticular thalamic and thalamocortical neurons: Scenario of sleep rhythm generation in interacting thalamic and neocortical networks. *The Journal of Neuroscience: The Official Journal of the Society for Neuroscience*, *13*(8), 3284–3299.

Steriade, M., Nuñez, A., & Amzica, F. (1993a). A novel slow (< 1 Hz) oscillation of neocortical neurons in vivo: Depolarizing and hyperpolarizing components. *The Journal of Neuroscience: The Official Journal of the Society for Neuroscience*, *13*(8), 3252–3265.

Steriade, M., Nuñez, A., & Amzica, F. (1993b). Intracellular analysis of relations between the slow (< 1 Hz) neocortical oscillation and other sleep rhythms of the electroencephalogram. *The Journal of Neuroscience: The Official Journal of the Society for Neuroscience*, *13*(8), 3266–3283.

Steriade, M., & Timofeev, I. (2003). Neuronal plasticity in thalamocortical networks during sleep and waking oscillations. *Neuron*, *37*(4), 563–576. https://doi.org/10.1016/s0896-6273(03)00065-5

Steriade, M., Timofeev, I., & Grenier, F. (2001). Natural waking and sleep states: A view from inside neocortical neurons. *Journal of Neurophysiology*, *85*(5), 1969–1985. https://doi.org/10.1152/jn.2001.85.5.1969

Stosiek, C., Garaschuk, O., Holthoff, K., & Konnerth, A. (2003). In vivo two-photon calcium imaging of neuronal networks. *Proceedings of the National Academy of Sciences*, *100*(12), 7319–7324. https://doi.org/10.1073/pnas.1232232100

Sun, J.-J., Kilb, W., & Luhmann, H. J. (2010). Self-organization of repetitive spike patterns in developing neuronal networks in vitro. *The European Journal of Neuroscience*, *32*(8), 1289–1299. https://doi.org/10.1111/j.1460-9568.2010.07383.x

Szabó, Z., Héja, L., Szalay, G., Kékesi, O., Füredi, A., Szebényi, K., Dobolyi, Á., Orbán, T. I., Kolacsek, O., Tompa, T., Miskolczy, Z., Biczók, L., Rózsa, B., Sarkadi, B., & Kardos, J. (2017). Extensive astrocyte synchronization advances neuronal coupling in slow wave activity in vivo. *Scientific Reports*, *7*(1), 6018. https://doi.org/10.1038/s41598-017-06073-7

Timofeev, I., & Chauvette, S. (2017). Sleep slow oscillation and plasticity. *Current Opinion in Neurobiology*, *44*, 116–126. https://doi.org/10.1016/j.conb.2017.03.019

Timofeev, I., Contreras, D., & Steriade, M. (1996). Synaptic responsiveness of cortical and thalamic neurones during various phases of slow sleep oscillation in cat. *The Journal of Physiology*, *494 (Pt 1)*, 265–278. https://doi.org/10.1113/jphysiol.1996.sp021489

Timofeev, I., Grenier, F., Bazhenov, M., Sejnowski, T. J., & Steriade, M. (2000). Origin of slow cortical oscillations in deafferented cortical slabs. *Cerebral Cortex (New York, N.Y.: 1991)*, *10*(12), 1185–1199. https://doi.org/10.1093/cercor/10.12.1185

Timofeev, I., Grenier, F., & Steriade, M. (2000). Impact of intrinsic properties and synaptic factors on the activity of neocortical networks in vivo. *Journal of Physiology, Paris*, *94*(5–6), 343–355. https://doi.org/10.1016/s0928-4257(00)01097-4

Timofeev, I., Grenier, F., & Steriade, M. (2001). Disfacilitation and active inhibition in the neocortex during the natural sleep-wake cycle: An intracellular study. *Proceedings of the National Academy of Sciences of the United States of America*, *98*(4), 1924–1929. https://doi.org/10.1073/pnas.041430398

Timofeev, I., Schoch, S. F., LeBourgeois, M. K., Huber, R., Riedner, B. A., & Kurth, S. (2020). Spatio-temporal properties of sleep slow waves and implications for

development. *Current Opinion in Physiology*, *15*, 172–182. https://doi.org/10.1016/j.cophys.2020.01.007

Tononi, G., & Cirelli, C. (2003). Sleep and synaptic homeostasis: A hypothesis. *Brain Research Bulletin*, *62*(2), 143–150. https://doi.org/10.1016/j.brainresbull.2003.09.004

Tononi, G., & Cirelli, C. (2014). Sleep and the Price of Plasticity: From Synaptic and Cellular Homeostasis to Memory Consolidation and Integration. *Neuron*, *81*(1), 12–34. https://doi.org/10.1016/j.neuron.2013.12.025

Vaidyanathan, T. V., Collard, M., Yokoyama, S., Reitman, M. E., & Poskanzer, K. E. (2021). Cortical astrocytes independently regulate sleep depth and duration via separate GPCR pathways. *ELife*, *10*, e63329. https://doi.org/10.7554/eLife.63329

Van Cauter, E., Leproult, R., & Plat, L. (2000). Age-related changes in slow wave sleep and REM sleep and relationship with growth hormone and cortisol levels in healthy men. *JAMA*, *284*(7), 861–868. https://doi.org/10.1001/jama.284.7.861

Vitiello, M. V., & Prinz, P. N. (1989). Alzheimer's disease. Sleep and sleep/wake patterns. *Clinics in Geriatric Medicine*, *5*(2), 289–299.

Vitiello, M. V., Prinz, P. N., Williams, D. E., Frommlet, M. S., & Ries, R. K. (1990). Sleep disturbances in patients with mild-stage Alzheimer's disease. *Journal of Gerontology*, *45*(4), M131-138. https://doi.org/10.1093/geronj/45.4.m131

Volgushev, M., Chauvette, S., Mukovski, M., & Timofeev, I. (2006). Precise Long-Range Synchronization of Activity and Silence in Neocortical Neurons during Slow-Wave Sleep. *The Journal of Neuroscience*, *26*(21), 5665–5672. https://doi.org/10.1523/JNEUROSCI.0279-06.2006

Walker, M. P. (2009). The role of slow wave sleep in memory processing. *Journal of Clinical Sleep Medicine: JCSM: Official Publication of the American Academy of Sleep Medicine*, *5*(2 Suppl), S20-26.

Wang, X., Arbel-Ornath, M., Wegmann, S. K., Kastanenka, K. V., & Bacskai, B. J. (2014). In Vivo Imaging in Neurodegenerative Diseases. In R. Weigert (Ed.), *Advances in Intravital Microscopy: From Basic to Clinical Research* (pp. 45–80). Springer Netherlands. https://doi.org/10.1007/978-94-017-9361-2_3

Wang, X., Kastanenka, K. V., Arbel-Ornath, M., Commins, C., Kuzuya, A., Lariviere, A. J., Krafft, G. A., Hefti, F., Jerecic, J., & Bacskai, B. J. (2018). An acute functional screen identifies an effective antibody targeting amyloid-β oligomers based on

calcium imaging. *Scientific Reports*, *8*(1), 4634. https://doi.org/10.1038/s41598-018-22979-2

Westerberg, C. E., Florczak, S. M., Weintraub, S., Mesulam, M.-M., Marshall, L., Zee, P. C., & Paller, K. A. (2015). Memory improvement via slow-oscillatory stimulation during sleep in older adults. *Neurobiology of Aging*, *36*(9), 2577–2586. https://doi.org/10.1016/j.neurobiolaging.2015.05.014

Westerberg, C. E., Mander, B. A., Florczak, S. M., Weintraub, S., Mesulam, M.-M., Zee, P. C., & Paller, K. A. (2012). Concurrent impairments in sleep and memory in amnestic mild cognitive impairment. *Journal of the International Neuropsychological Society: JINS*, *18*(3), 490–500. https://doi.org/10.1017/S135561771200001X

Whitaker, M. (2010). Genetically encoded probes for measurement of intracellular calcium. *Methods in Cell Biology*, *99*, 153–182. https://doi.org/10.1016/B978-0-12-374841-6.00006-2

Winer, J. R., Mander, B. A., Helfrich, R. F., Maass, A., Harrison, T. M., Baker, S. L., Knight, R. T., Jagust, W. J., & Walker, M. P. (2019). Sleep as a Potential Biomarker of Tau and β-Amyloid Burden in the Human Brain. *The Journal of Neuroscience: The Official Journal of the Society for Neuroscience*, *39*(32), 6315–6324. https://doi.org/10.1523/JNEUROSCI.0503-19.2019

Wu, J. W., Hussaini, S. A., Bastille, I. M., Rodriguez, G. A., Mrejeru, A., Rilett, K., Sanders, D. W., Cook, C., Fu, H., Boonen, R. A. C. M., Herman, M., Nahmani, E., Emrani, S., Figueroa, Y. H., Diamond, M. I., Clelland, C. L., Wray, S., & Duff, K. E. (2016). Neuronal activity enhances tau propagation and tau pathology in vivo. *Nature Neuroscience*, *19*(8), 1085–1092. https://doi.org/10.1038/nn.4328

Xie, L., Kang, H., Xu, Q., Chen, M. J., Liao, Y., Thiyagarajan, M., O'Donnell, J., Christensen, D. J., Nicholson, C., Iliff, J. J., Takano, T., Deane, R., & Nedergaard, M. (2013). Sleep drives metabolite clearance from the adult brain. *Science (New York, N.Y.)*, *342*(6156), 373–377. https://doi.org/10.1126/science.1241224

Yamamoto, K., Tanei, Z.-I., Hashimoto, T., Wakabayashi, T., Okuno, H., Naka, Y., Yizhar, O., Fenno, L. E., Fukayama, M., Bito, H., Cirrito, J. R., Holtzman, D. M., Deisseroth, K., & Iwatsubo, T. (2015). Chronic optogenetic activation augments aβ pathology in a mouse model of Alzheimer disease. *Cell Reports*, *11*(6), 859–865. https://doi.org/10.1016/j.celrep.2015.04.017

Yang, G., Lai, C. S. W., Cichon, J., Ma, L., Li, W., & Gan, W.-B. (2014). Sleep promotes branch-specific formation of dendritic spines after learning. *Science (New York, N.Y.)*, *344*(6188), 1173–1178. https://doi.org/10.1126/science.1249098

Zielinski, M. R., Atochin, D. N., McNally, J. M., McKenna, J. T., Huang, P. L., Strecker, R. E., & Gerashchenko, D. (2019). Somatostatin+/nNOS+ neurons are involved in delta electroencephalogram activity and cortical-dependent recognition memory. *Sleep*, *42*(10), zsz143. https://doi.org/10.1093/sleep/zsz143

Zucca, S., Pasquale, V., Lagomarsino de Leon Roig, P., Panzeri, S., & Fellin, T. (2019). Thalamic Drive of Cortical Parvalbumin-Positive Interneurons during Down States in Anesthetized Mice. *Current Biology*, *29*(9), 1481-1490.e6. https://doi.org/10.1016/j.cub.2019.04.007

CURRICULUM VITAE